SfB Jd:Gi:df2
UDC 620.19:624.072.2.012.45

RESEARCH REPORT **18** *PART 1*

An investigation of the crack control characteristics of various types of bar in reinforced concrete beams

CEMENT AND CONCRETE ASSOCIATION

RESEARCH REPORT 18, Part 1: DECEMBER 1966

AN INVESTIGATION OF THE CRACK CONTROL CHARACTERISTICS OF VARIOUS TYPES OF BAR IN REINFORCED CONCRETE BEAMS

G. D. Base, BSc (Eng), AMICE, J. B. Read,
A. W. Beeby, BSc (Eng), AMICE and H. P. J. Taylor, BSc (Tech)

SUMMARY

An investigation, sponsored by the Civil Engineering Research Association, into the factors influencing the width and distribution of cracks in zones of uniform bending moment in reinforced concrete flexural members incorporating various types of bar, is described. In tests on 133 beams nearly a quarter of a million crack measurements were made and analysed.

It was shown that the distribution of cracks in a beam was Gaussian and that the standard deviation of the crack widths averaged 0·42 of the mean crack width; approximately one crack in a hundred thus exceeded a width of twice the mean crack width.

The principal factors determining crack width on the surface of the effective tension zone of a beam were shown to be the distance from the point of measurement of the crack to the surface of the nearest reinforcement bar and the distance from the neutral axis of the beam.

The type of bar (whether plain round, square twisted or ribbed) and the size of bar (within the range $\frac{1}{2}$ in. to $1\frac{1}{4}$ in.) had little influence on cracking.

The following hypothesis would explain the results of the investigation. Within the range of crack widths normally considered acceptable in reinforced concrete, adhesion between the reinforcement and the concrete does not break down significantly and crack width is primarily a function of the elastic recovery of the concrete between cracks and of the restraining influence of the nearby reinforcement. Cracks taper from a certain width on the surface of a beam to near zero width at the steel-concrete interface.

The investigation results in the following formula for the prediction of the maximum crack width on the surface of the effective tension zone in a region of uniform bending moment in a beam:

$$\omega_{max} = Kc \frac{f_s}{E_s} \left(\frac{d - d_n}{d_1 - d_n} \right)$$

where c = *the distance of the point of measurement of the crack from the surface of the nearest reinforcement bar;*

d = *the distance of the point of measurement of the crack from the compression face of the section;*

d_1 = *the distance of the centroid of the reinforcement from the compression face of the section;*

d_n = *the distance of the neutral axis from the compression face of the section;*

f_s = *the mean stress in the reinforcement;*

E_s = *the modulus of elasticity of the reinforcement; and*

K = *a constant of value 3·3 for deformed bars (ribbed or square twisted) and 4·0 for plain round bars.*

Part 1 of this report discusses the findings of the initial series of tests on 105 beams. The detailed test results from these 105 beams are given in the form of diagrams in the separately published supplement to Part 1; the findings of an additional programme of tests on a further 28 beams will be published as Part 2 of the report.

Introduction

Very many investigations of the phenomenon of bond between the concrete and the steel in reinforced concrete beams have been carried out since 1878. Hundreds of patents have been issued for deformed bars but it is only in comparatively recent years that deformed bars (with the exception of square twisted bars) have been widely used in this country.

Most of the experimental and theoretical research on bond has been directed towards an understanding of two basic aspects of the problem: the anchorage

length required at the end of a reinforcing bar in various situations; and the factors governing the magnitude and distribution of cracks in the body of a beam, particularly in zones of constant bending moment. However, despite the amount of work carried out, the phenomenon is still far from being completely understood and reliable design data are lacking.

It has generally been assumed that the two aspects of the problem are related and that better anchorage properties in a bar automatically ensure better crack control characteristics. This assumption has possibly been a factor contributing to the preponderance of research effort on what is generally considered to be the more amenable aspect of the research problem—the anchorage length.

As indicated in the next section, there might, indeed, be little or no connexion between the two aspects and an extensive effort to investigate, directly, the factors governing crack control is essential.

The parameters that might influence cracking are numerous and include the following:

(1) stress in the reinforcement;
(2) surface characteristics of the reinforcement;
(3) size of the reinforcing bars;
(4) percentage of reinforcement in the total beam cross section;
(5) degree of concentration of the reinforcement within the tension zone of the beam. This gives rise to the parameter p_e, the ' effective reinforcement ratio ' defined as the ratio of the total cross sectional area of the reinforcement to the area of concrete, A_e, with the same centroid as the reinforcement;
(6) the area of concrete associated with individual reinforcing bars;
(7) the cover to the bars;
(8) the strength of the concrete;
(9) the degree of compaction of the concrete achieved around the bars;
(10) the deformability of the concrete;
(11) the type of concrete, particularly aggregate type and cement type;
(12) the curing conditions of the concrete;
(13) the positioning of stirrups;
(14) the method of loading.

Complicated interaction of some of these parameters occurs and it is not possible to investigate each one separately. Successful investigation of them is only possible in a programme designed to isolate those parameters that can be isolated and to compare, in as many ways as possible, the effects of groups of interacting parameters so that the predominent parameters are determined. Such a programme must clearly be very extensive and has not, to date, been reported. The investigation described in this report is, however, considerably more extensive than any previously reported work.

Possible mechanisms of crack formation

The basic concepts regarding the mechanism of crack formation used in most previous studies have been closely similar and the basic mathematical expressions developed for crack width and spacing have therefore also been similar. General equations were given by Watstein and Parsons in 1943[1] and several other theories, differing primarily in the distribution assumed for local bond stress, are given in the published proceedings of the RILEM Symposium on bond and crack formation in reinforced concrete[2]. Commission IVa on Cracking, of the European Concrete Committee (CEB), has attempted a synthesis of various theories. The basic concepts used by the CEB, which are common to most individual theories, are as follows.

1: 'CLASSICAL' THEORY OF THE MECHANISM OF CRACK FORMATION

In a reinforced concrete member loaded in axial tension (Figure 1a), cracks will form when the tensile strength of the concrete is exceeded. The first cracks (A and C) will be at the weakest sections, which will be randomly spaced. Similarly, in a beam loaded in bending (Figure 1b), initial cracks (A and C) will form when the modulus of rupture is exceeded at weak sections. At higher loads further cracks (B) will form between the initial ones but the crack spacing can only be reduced to a certain minimum value, S_{min}, which is reached when a tensile force of sufficient magnitude to form an additional crack between two existing cracks can no longer be transmitted by bond from the steel to the concrete.

Crack formation is inherently subject to far greater variation than such properties of concrete as tensile or compressive strength. If two cracks form initially with a spacing slightly greater than $2S_{min}$ then another crack may later form between them. However, if two initial cracks form at a spacing slightly less than $2S_{min}$ then a new crack cannot form. Thus, basically, crack spacing may be expected to vary from S_{min} to $2S_{min}$ with an average spacing of $1{\cdot}5S_{min}$ so that $S_{max} = \frac{4}{3}S_{ave}$ and $S_{min} = \frac{2}{3}S_{ave}$

To develop mathematical expressions for minimum crack spacing it is considered that tension sufficient to form a new crack at B (Figure 1) is transferred by bond from steel to concrete between A and B. Then concrete tensile strength = transferred tension, i.e.

$$A_e f_t = S_{min} r_1 u \Sigma o \quad \ldots\ldots\ldots\ldots (1)$$

where A_e = effective concrete area in tension
f_t = tensile strength of concrete
S_{min} = minimum crack spacing
r_1 = factor defining distribution of bond stress
u = maximum bond stress
Σo = sum of bar perimeters.

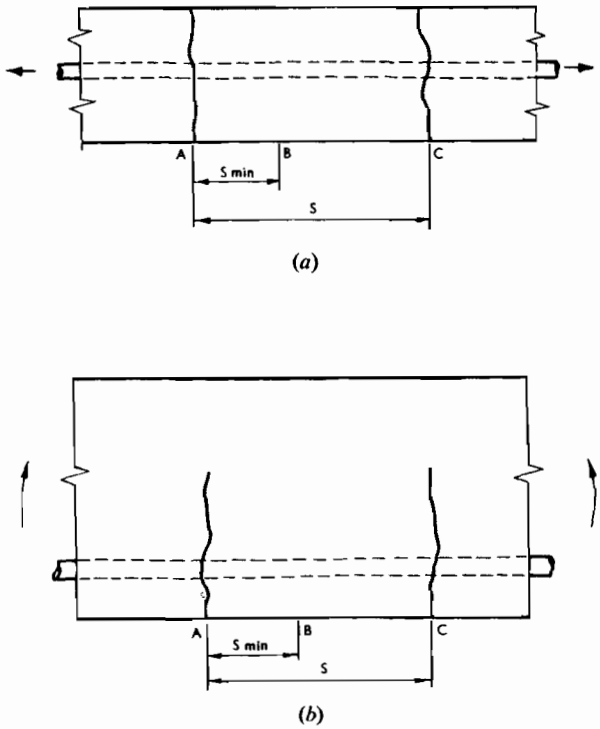

Figure 1: Mechanism of cracking—'classical' theory.

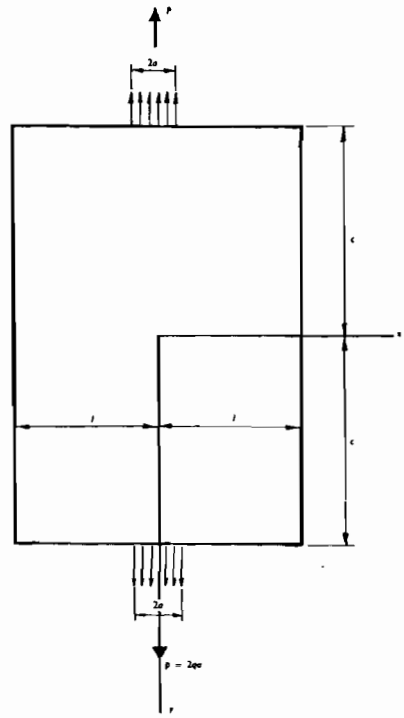

Figure 2: Mechanism of cracking—elastic model for the 'no slip' theory.

Substituting $S_{max} = 2S_{min}$ gives

$$S_{max} = \frac{2f_t A_e}{r_1 u \Sigma o} \quad \ldots\ldots\ldots\ldots\ldots\ldots (2)$$

Substituting $\Sigma o = \frac{4A_s}{D}$ and $p_e = \frac{A_s}{A_e}$ gives

$$S_{max} = \frac{f_t D}{2r_1 u p_e} \quad \ldots\ldots\ldots\ldots\ldots\ldots (3)$$

where A_s = area of reinforcement
D = bar diameter
p_e = effective reinforcement ratio.

The maximum crack width, ω_{max}, is assumed to be the elongation of the steel between two cracks minus the elongation of the concrete. In the CEB general theory[3] the elongation of the concrete is neglected so that $\omega_{max} = S_{max} \frac{f_s}{E_s}$, which gives

$$\omega_{max} = \frac{D f_s}{p_e K_1} \quad \ldots\ldots\ldots\ldots\ldots\ldots (4)$$

where ω_{max} = maximum crack width

$K_1 = 2r_1 u \frac{E_s}{f_t}$

f_s = stress in reinforcement.

Expression 4 states inverse proportionality between ω_{max} and p_e but European test data indicate that this is an over-emphasis of the effect of p_e. Thus the following modified expression has been adopted by the CEB:

$$\omega_{max} = \left(4{\cdot}5 + \frac{0{\cdot}40}{p_e}\right) D \frac{f_s}{K_2} \quad \ldots\ldots\ldots\ldots (5)$$

where K_2 is a coefficient depending on the bond characteristics of the reinforcement and is determined experimentally.

This approach thus assumes that cracks are produced by slip of the concrete relative to the reinforcement; that the crack spacing is governed by the force that can be transmitted from the steel to the concrete and, thus, by the bond characteristics of the steel; and that the crack is approximately uniform in width between the steel and side of the beam.

2: 'NO SLIP' THEORY OF THE MECHANISM OF CRACK FORMATION

This approach is fundamentally different from the 'classical' theory in that it assumes that, for the range of crack widths normally permitted in reinforced concrete, there is no slip of the steel relative to the adjacent concrete. The crack is thus assumed to be of zero width at the steel-concrete interface and to increase in width towards the face of the beam. The crack width is essentially a function of the elastic strain of the concrete.

Considering, as a simplified model of the problem, a concentrated load applied to a section as in Figure 2, we have the basic expression[4]:

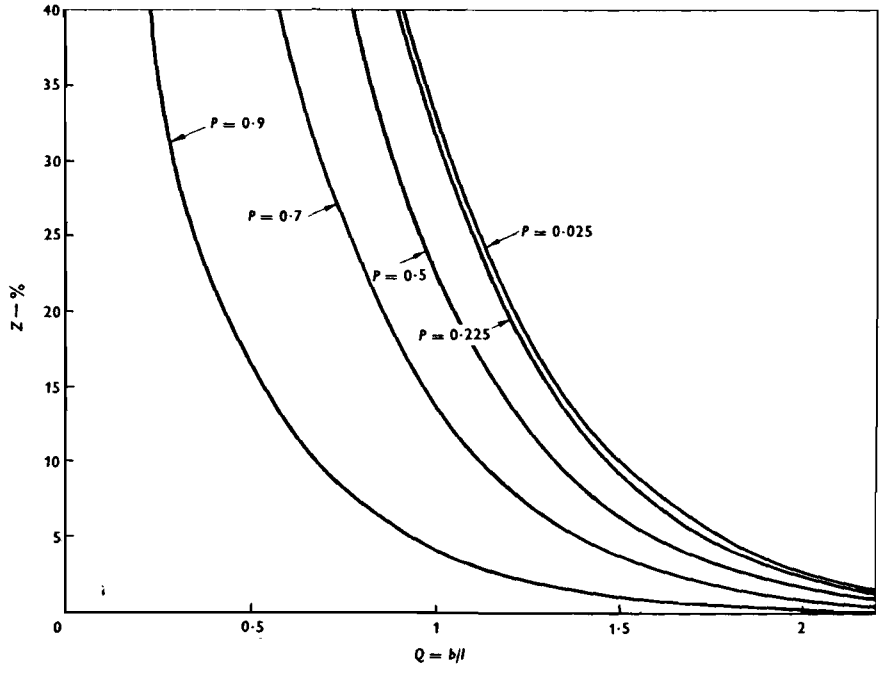

Figure 3: 'No slip' theory. Relationship between Z and Q for various values of P.

$$\sigma_y = \frac{qa}{l} + \frac{4q}{\pi} \sum_{m=1}^{\infty} \frac{\sin \alpha a}{m} \times \left(\frac{(\alpha c \cosh \alpha c + \sinh \alpha c) \cosh \alpha y - \alpha y \sinh \alpha y \sinh \alpha c}{\sinh 2\alpha c + 2\alpha c} \right) \times \cos \alpha x$$

for values of $\zeta \geqslant 2$, $\cosh \zeta = \sinh \zeta = \frac{1}{2} e^{\zeta}$ to within 2%.

Thus, for all reasonable values of c, l and y we can write:

$$\sigma_y = \frac{qa}{l} + \frac{4q}{\pi} \sum_{m=1}^{\infty} \frac{\sin \alpha a}{m} \times \left(\frac{\left(\frac{\alpha c e^{\alpha c}}{2} + \frac{e^{\alpha c}}{2} \right) \frac{1}{2} e^{\alpha y} - \left(\frac{1}{4} \alpha y e^{\alpha y} e^{\alpha c} \right)}{\frac{1}{2} e^{2\alpha c} + 2\alpha c} \right) \cos \alpha x$$

Further, the term $2\alpha c$ is generally small compared with $\frac{1}{2} e^{2\alpha c}$ and the equation finally simplifies to

$$\sigma_y = \frac{qa}{l} + \frac{4q}{\pi} \sum_{m=1}^{\infty} \frac{\sin \alpha a}{2m} \left(\frac{1 + \alpha b}{e^{\alpha b}} \right) \cos \alpha x$$

where $b = c - y$ = distance from one end of the block.

As b increases $\sigma_y \rightarrow \frac{qa}{e}$ since $\frac{1 + \alpha b}{e^{\alpha b}} \rightarrow 0$.

At a crack the stress, σ_y, on the face of the concrete specimen must be zero. Moving away from the crack the stress σ_y increases until the stress through the section is uniform. A second surface crack is unlikely to occur until the surface stress has built up to nearly the maximum value. It is thus necessary to determine the rate at which the term

$$\frac{4q}{\pi} \sum_{m=1}^{\infty} \frac{\sin \alpha a}{2m} \left(\frac{1 + \alpha b}{e^{\alpha b}} \right) \cos \alpha x$$

approaches zero at the surface of the specimen, i.e. when $x = l$.

Considering, therefore, the function

$$Z = \frac{\frac{4q}{\pi} \sum_{m=1}^{\infty} \frac{\sin \alpha a}{2m} \left(\frac{1 + \alpha b}{e^{\alpha b}} \right) \cos m\pi}{\frac{qa}{l}} \times 100\%$$

if we let $\frac{a}{l} = P$ and $\frac{b}{l} = Q$ we have

$$Z = \frac{400}{\pi P} \sum_{m=1}^{\infty} \frac{\sin m\pi P}{2m} \left(\frac{1 + m\pi Q}{e^{m\pi Q}} \right) \cos m\pi$$

Plotting Z against Q for various values of P gives the curves in Figure 3.

In a direct tension specimen it seems likely that further cracking will occur when the surface stress approaches the maximum value very closely, i.e. when $Z \rightarrow 0$. In a flexural specimen, however, bending stress will be superimposed on the direct stresses considered in this simplified approach to the problem. In beams of the proportions used in the investigation covered in this report the bending stress at the extreme fibres will be approximately 115% of the stress at the steel level. Thus it seems logical to consider a value of $Z = 15$ as the criterion governing the formation of further surface cracks between existing cracks. If P is plotted against Q for $Z = 15$ the curve in Figure 4 is obtained.

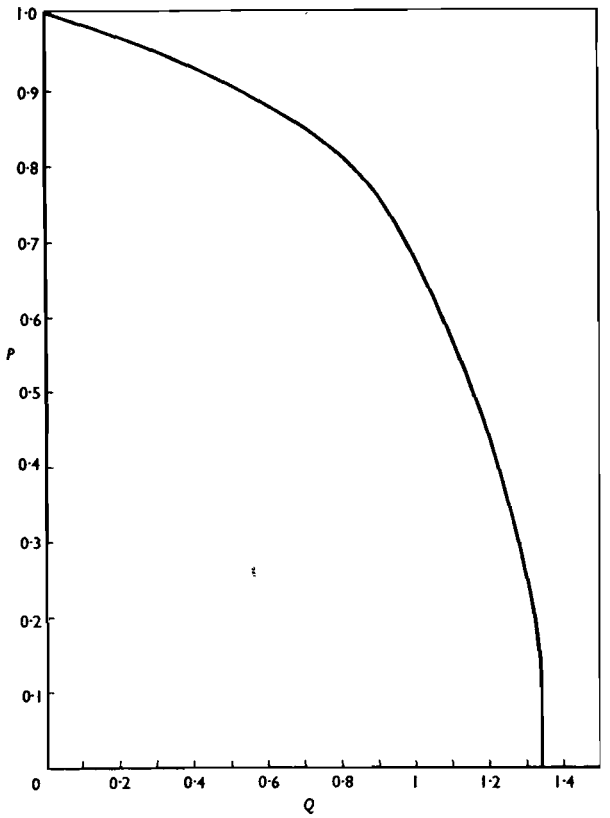

Figure 4: 'No slip' theory. Relationship between P and Q for Z = 15.

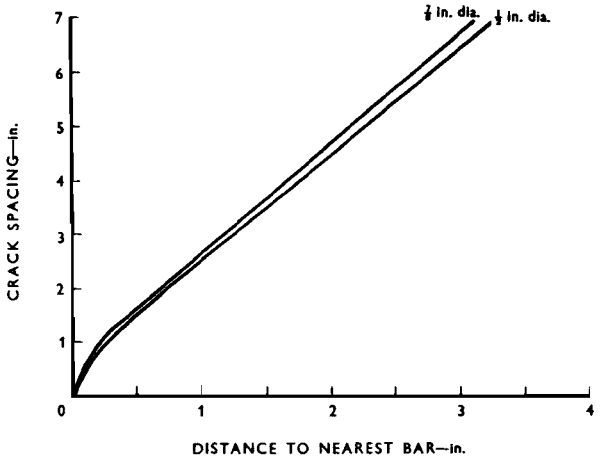

Figure 5: 'No slip' theory of cracking—predicted crack spacing.

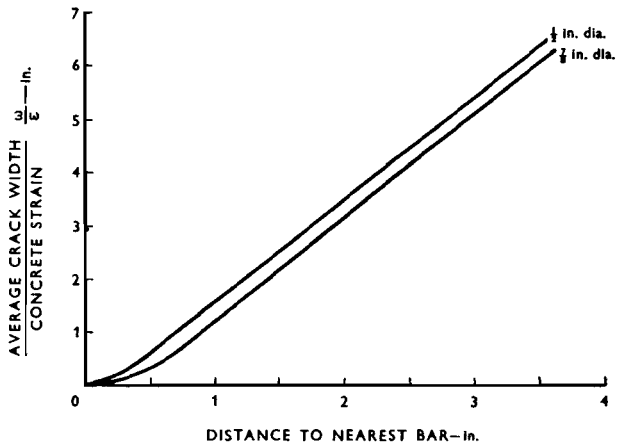

Figure 6: 'No slip' theory of cracking—predicted crack widths.

From this can be obtained the relationships between crack spacing and the distance of the point of measurement of the crack from the nearest bar, as shown in Figure 5. Such relationships will later be compared with the experimental results. It can be seen that an almost direct proportionality between crack spacing and cover is predicted.

Extension of this elastic theory can be used to predict proportionality between crack width and cover to the reinforcement[5] (Figure 6). A more refined theoretical approach in which the force is considered to be transferred from the steel to the concrete along the surface of the bar may seem desirable but would clearly require assumptions as to the bond stress distribution.

The basic assumptions of this mechanism of cracking, based on the theory of elasticity, is that there is no slip between the steel and the concrete at primary cracks, i.e. cracks visible on the beam surface. It seems likely, however, that there will also be micro-cracking of the restrained concrete near the steel-concrete interface, particularly in the highly strained concrete on either side of a primary crack, and that the sum of the widths of these micro-cracks will be similar to the sum of the widths of the primary cracks at the surface of the beam. As the steel stress increases to large values it is probable that the micro-cracks will widen and complete bond break-down between the steel and concrete will follow. However, we are interested primarily in the range of steel stresses used in current practice, or likely to be used in the forseeable future, and should limit our considerations to these stresses.

Basis of programme of tests

The large number of parameters involved clearly makes a statistical approach to the problem of cracking a formidable task. However, previous research work and generally accepted ideas indicated that certain of the parameters have a very strong influence on cracking. For example, from the extensive series of tests carried out by the Portland Cement Association and reported by Hognestad[6], the following are included in the major findings.

" The use of modern American deformed bars is a

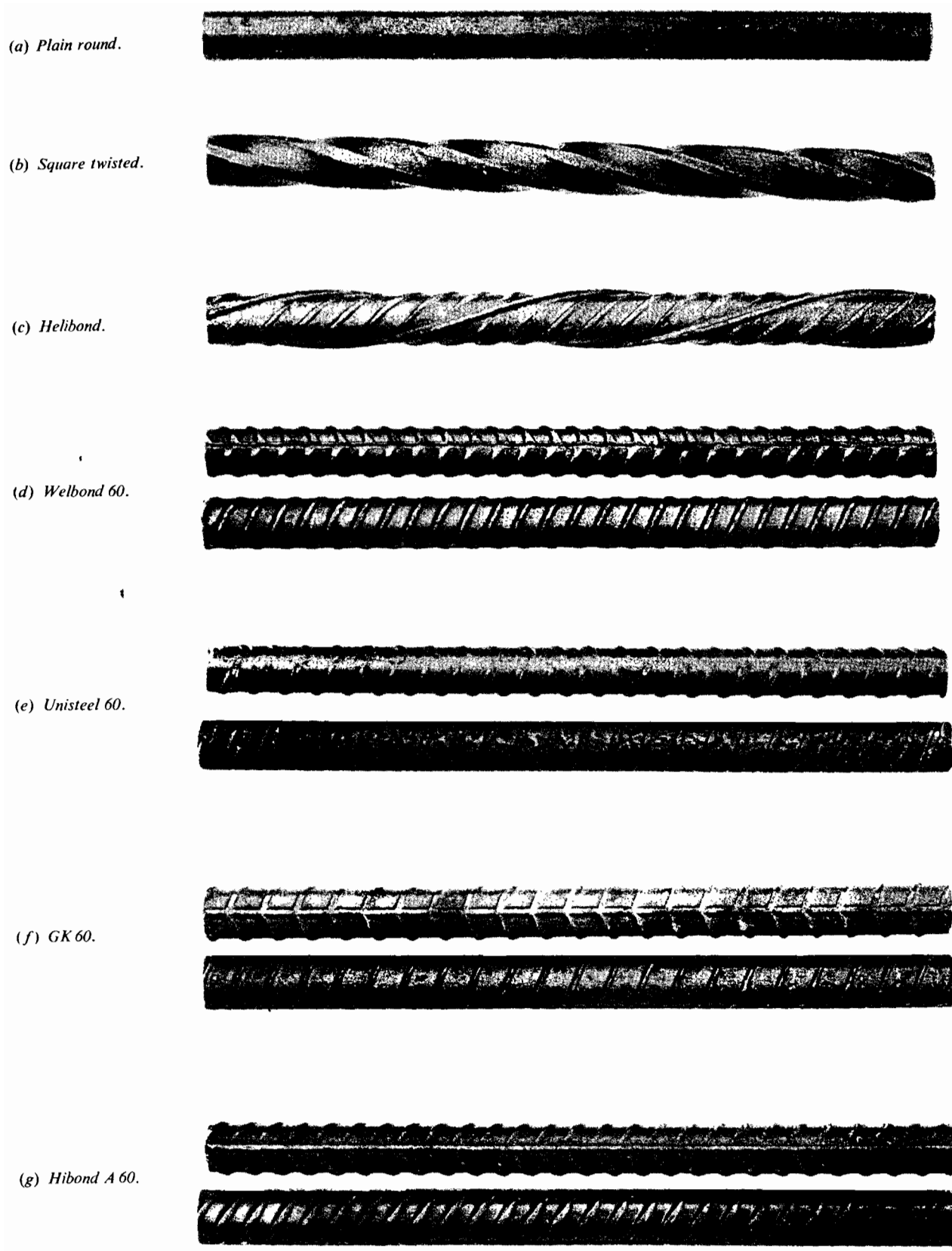

Figure 7: Typical reinforcing bars used in the investigation.

TABLE 1: **Details of deformations of typical steels.**

Bar type	Diameter (in.)	Longitudinal deformation	Width (in.)	Height or depth (in.)	Lateral deformation	Spacing (in.)	Length (in.)	Width (in.)	Height (in.)
Helibond	0·500	Helical rib 3 in. pitch	0·028	0·062	Rib	0·350	1·190	0·046	0·026
Helibond	0·875	Helical rib 5 in. pitch	0·078	0·088	Rib	0·700	2·000	0·078	0·045
Helibond	1·250	Helical rib 7 in. pitch	0·118	0·088	Rib	0·875	2·250	0·110	0·090
Unisteel 60	0·500	None	—	—	Rib	0·340	0·700	0·055	0·026
Unisteel 60	0·875	None	—	—	Rib	0·562	1·375	0·093	0·032
Unisteel 60	1·250	None	—	—	Rib	0·812	1·812	0·125	0·057
Welbond 60	0·500	Groove	0·078	0·012	Rib	0·270	0·750	0·062	0·040
Welbond 60	0·875	Groove	0·063	0·011	Rib	0·475	1·375	0·071	0·060
Welbond 60	1·250	Groove	0·125	0·018	Rib	0·613	1·750	0·125	0·056
G.K.60	0·500	Rib	0·078	0·033	Rib	0·330	0·750	0·038	0·021
G.K.60	0·625	Rib	0·078	0·054	Rib	0·420	1·000	0·047	0·030
G.K.60	0·750	Rib	0·075	0·058	Rib	0·510	1·180	0·062	0·044
G.K.60	0·875	Rib	0·075	0·060	Rib	0·600	1·500	0·062	0·053
Hi Bond A	0·875	Rib	0·087	0·057	Rib	0·440	1·190	0·100	0·057

highly effective crack control measure. Crack width for such deformed bars is less than one half of that for plain bars.

" Crack width is essentially proportioned to bar diameter, D, for plain bars and old-type American deformed bars, but less dependent on bar diameter for modern American deformed bars.

" The more recent CEB equation 7 predicts the crack width reasonably well for modern American deformed bars. However, equation 7 tends to over-emphasize effects of bar diameter and effective reinforcement ratio."

CEB equation 7 is the equation 5 in this report and indicates a very strong influence on crack widths of bar diameter and bar type. The influence of bar type is governed by the factor K_2 and a ratio 1:1·6 for plain and deformed bars was assumed.

The more highly deformed steels available in Britain are very similar to modern American deformed bars. It was therefore anticipated that the two parameters, bar size and bar type, would prove as important in Britain as in America.

The inherent variability of crack width within a beam has already been discussed and it was clear that, for statistical reasons, measurement of a considerable number of crack widths and spacings in each beam would be essential. A constant moment zone 80 in. long was therefore used in most tests and at least 20 cracks usually occurred in this zone.

Variability between similar beams was also expected to be considerable but, particularly for the parameters bar type and bar size, it was expected that comparatively small, well-controlled groups of comparison tests could be used to show the effect of parameters.

The basis of the programme was therefore the investigation, within groups of six beams cast and tested under uniform conditions, of the effect of varying a single parameter. Where parameters could not be separated, several groups of beams were used with the inter-related parameters varied in different ways.

Variables investigated

1: BAR TYPE

Of the large number of bars available in this country only a limited number could be included in the test programme. The bars used were chosen as representative of the range of bars available and were classified as follows.

(a) Plain round: in the majority of cases mild steel was used but in some cases steel with higher tensile properties was used.
(b) Square twisted, cold worked: bars with the same cross-sectional area as the round bars were used.
(c) Deformed, cold worked: only one such steel appeared to be available at the time of testing.
(d) Heavily deformed, hot rolled: a number of steels fitted into this classification and choice of the actual steels used was quite arbitrary.
(e) Lightly deformed, hot rolled: a number of steels fitted into this classification and, again, choice of the actual steel used was arbitrary.

All steels were used in a condition approximating to the ' as milled ' condition. Any light rusting that occurred during transit was removed by wire brushing before use. Figure 7 shows typical steels used in the investigation and Table 1 gives information regarding rib details for typical steels.

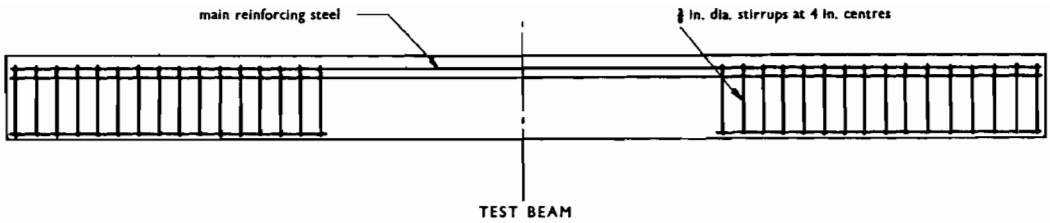

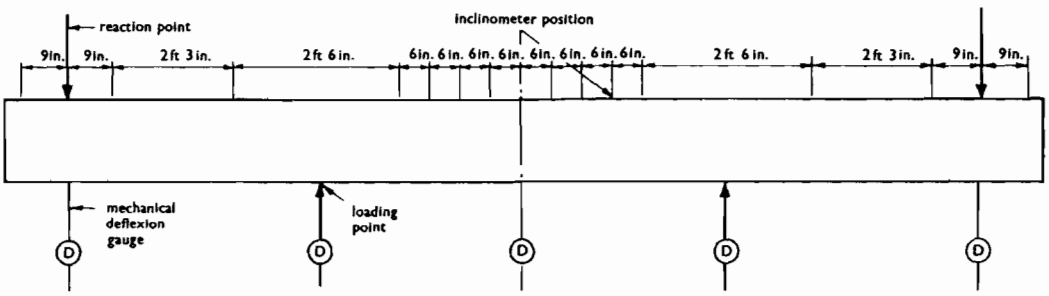

INCLINOMETERS AND DEFLEXION GAUGES

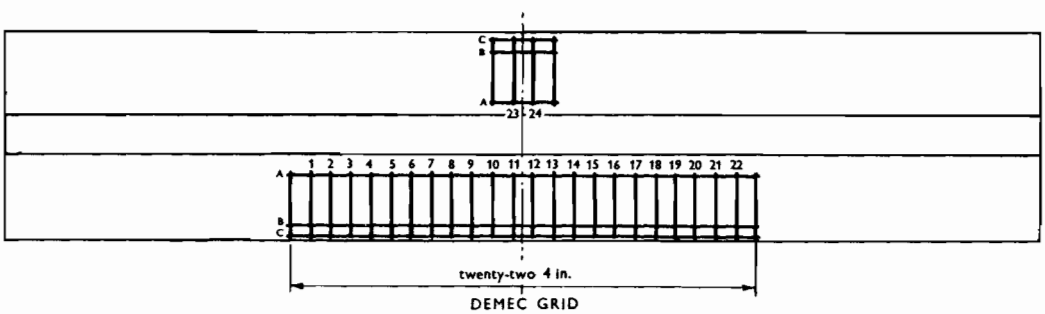

DEMEC GRID

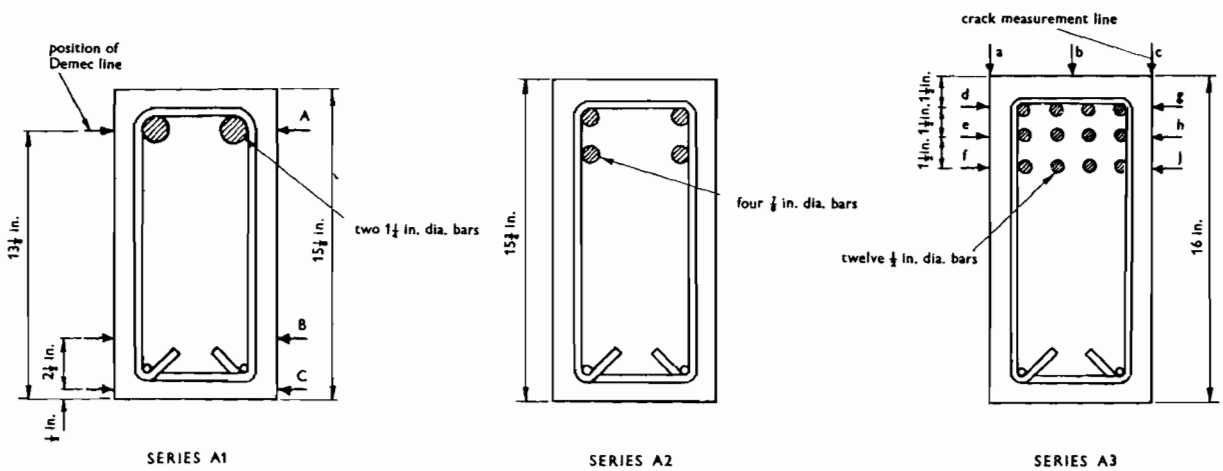

SERIES A1 SERIES A2 SERIES A3

Figure 8: Details of beams in Series A1, A2 and A3.

The first 36 beams tested were cast in six lots, each of six beams. In each casting there was one beam with each of the above five types of steel and the sixth beam was a duplicate of one of the five.

Equal cross-sectional areas of the various types of steel were used and comparison was made at similar stresses. Figure 8 shows the details of the beams, including the instrumentation.

2: BAR SIZE

For the basic investigation of this parameter three sizes of bar were used, namely those with cross-sectional areas equivalent to $\frac{1}{2}$ in., $\frac{7}{8}$ in. and $1\frac{1}{4}$ in. diameter bars. Of the first six castings, two were with $\frac{1}{2}$ in., two with $\frac{7}{8}$ in. and two with $1\frac{1}{4}$ in. bars and comparison was made between castings. Total cross-sectional areas of steel were maintained almost constant; either twelve $\frac{1}{2}$ in. bars (2·35 in^2), four $\frac{7}{8}$ in. bars (2·40 in^2) or two $1\frac{1}{4}$ in. bars (2·45 in^2) were used (Figure 8). Effective depth and width of beam, bottom and side cover to bars and stirrup details in the shear spans were intended to be identical. However, an error in bottom cover occurred in the casting of the beams with $\frac{1}{2}$ in. bars and must be allowed for in the comparisons of results.

3: SIDE COVER TO REINFORCEMENT

Variation of side cover to reinforcement can be made in several ways and other parameters are involved. These are illustrated in Figure 9. In Figure 9a, four $\frac{7}{8}$ in. bars at normal spacing and in rectangular layout are given various amounts of side cover. The cross-sectional area of concrete associated with each bar is thus varied considerably, as is the effective reinforcement ratio, p_e. In Figure 9b, twelve $\frac{1}{2}$ in. bars at normal spacing, in rectangular layout, are given various amounts of side cover. The variation in concrete area per bar and in p_e is considerably less pronounced in this series. Finally, in Figure 9c, four $\frac{7}{8}$ in. bars are grouped in three different ways within the same area of concrete. Six beams were cast in each series, half with plain round bars and half with heavily deformed bars. Variants of the series illustrated in Figures 9a and 9b were then made, with half as many reinforcing bars and with deformed steel only.

4: BOTTOM COVER TO REINFORCEMENT

Bottom cover to a rectangular layout of four $\frac{7}{8}$ in. bars was varied between $\frac{1}{2}$ in. and $2\frac{3}{4}$ in. as in Figure 10. All other details of the beams were maintained constant.

5: STIRRUPS IN THE CONSTANT MOMENT ZONE

Because it was suspected that stirrups would influence the formation of cracks, generally no stirrups were used in the constant moment zones of the test beams. It was intended to investigate the effect of stirrups by comparing beams with no stirrups in the constant moment zone with beams with stirrups at spacings of $\frac{2}{3}$ and $1\frac{1}{2}$ times the average crack spacing observed in beams without stirrups. However, normal crack spacing was so small that stirrup spacing at $\frac{2}{3}$ times the crack spacing would have been absurd. The influence of concrete cover to the stirrups was suspected to be important and therefore two groups of four beams were cast, one with plain bars and one with deformed bars; two beams in each casting had a small side and bottom cover to the stirrups while two beams had larger side and bottom cover. All eight beams had $\frac{3}{8}$ in. diameter mild steel stirrups at 6 in. centres in the constant moment zone; 6 in. was approximately $1\frac{1}{2}$ times normal crack spacing.

6: PERCENTAGE REINFORCEMENT AND EFFECTIVE REINFORCEMENT RATIO

The quantity of reinforcement in a beam can be varied by changing either the bar size or the number of bars. Changing the bar size produces a rapid change in the cross-sectional area of steel but a slow change in the surface area of the steel and in the cross-sectional area of concrete associated with each bar. Changing the number of bars produces similar rates of change in bar cross-sectional area, in bar surface area and in the cross-sectional area of concrete associated with each bar. Both methods of varying the reinforcement were used in the investigation (Figure 11). Two castings, each of six beams, were made, one with plain round bars and one with deformed bars. In three of the beams in each casting the reinforcement was varied by changing the number of bars (twelve, nine and six $\frac{1}{2}$ in. bars) and in the other three the bar size was changed (four $\frac{7}{8}$, $\frac{3}{4}$ and $\frac{5}{8}$ in. bars). Cover to the bars, the beam width and effective depth were kept constant.

7: LENGTH OF SHEAR SPAN

Because there is some indication from previous work that the length of the shear span has an influence on the cracking in the constant moment zone of a beam, three beams were tested with three different shear spans (30, 42 and 60 in. shear spans and 120, 96 and 60 in. constant moment zones respectively).

8: CONCRETE STRENGTH

This was varied in two ways. Three beams were cast with different compacting factors (obtained by varying water content) and then tested at approximately the same age and three beams were cast together under similar conditions and tested at different ages.

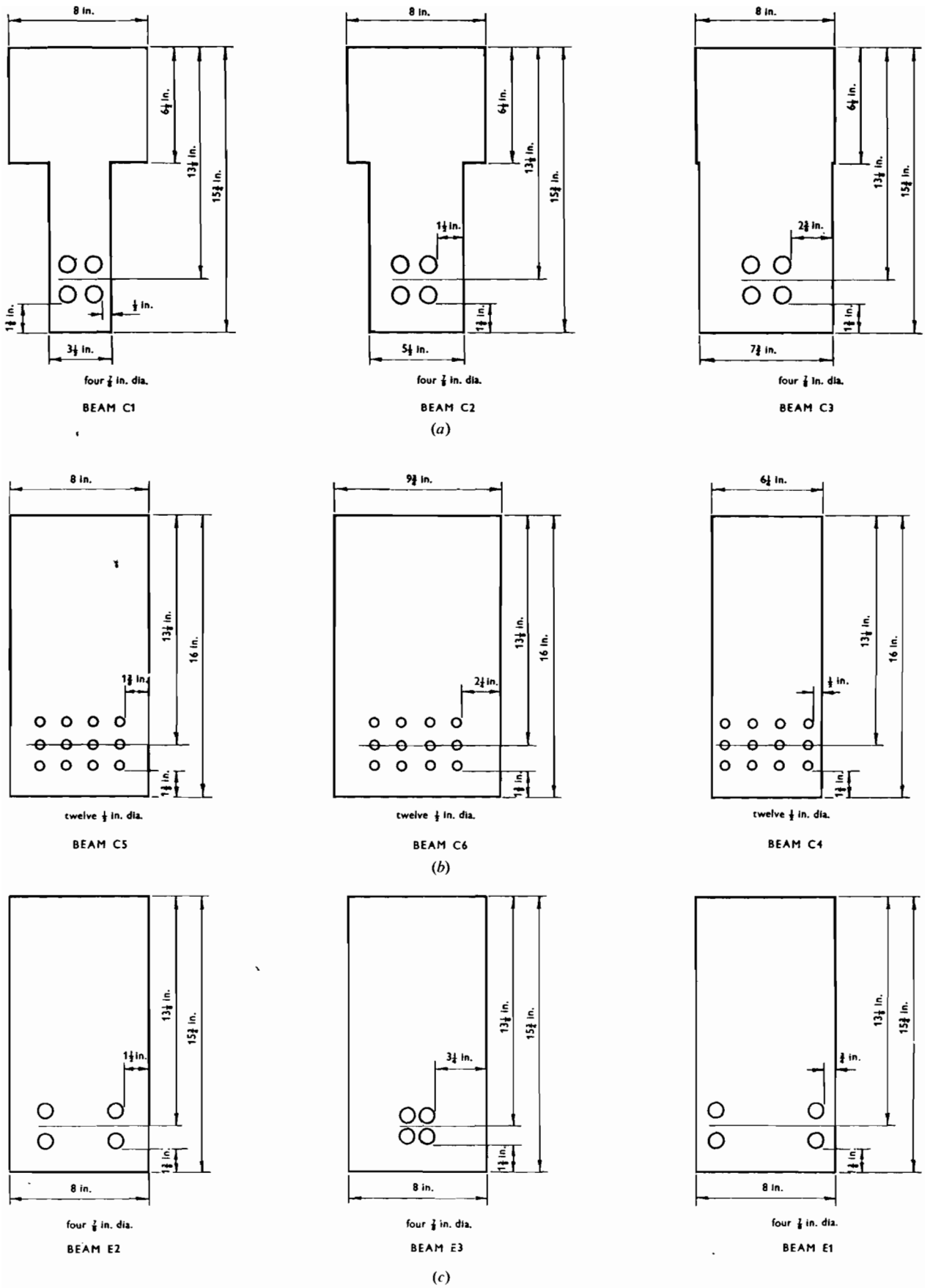

Figure 9: Beams for investigation of side cover to reinforcement.

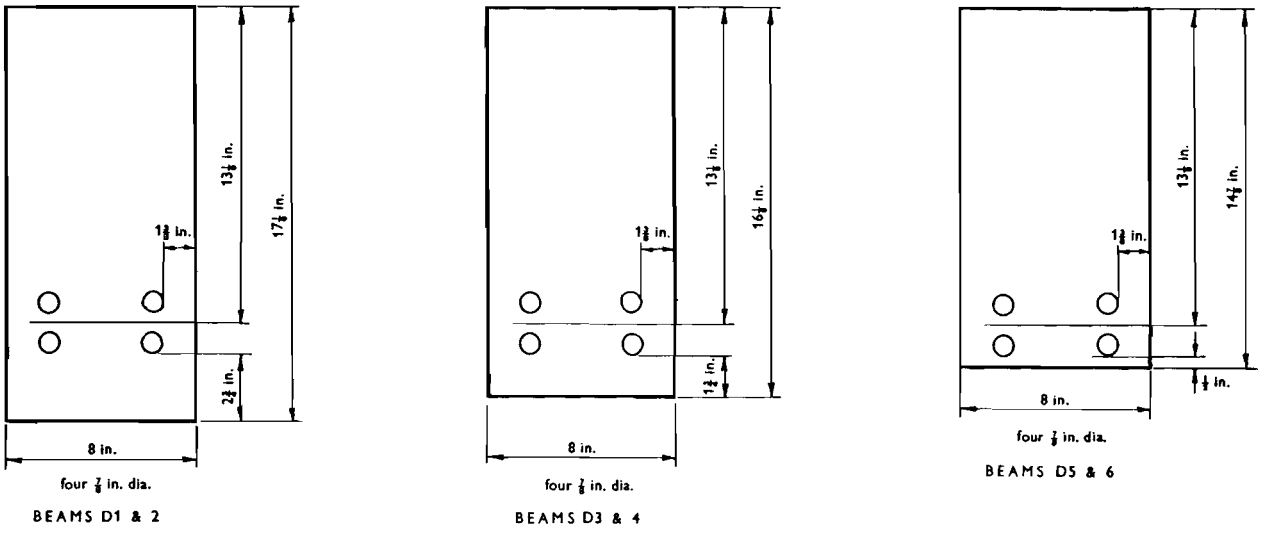

Figure 10: Beams for investigation of bottom cover to reinforcement.

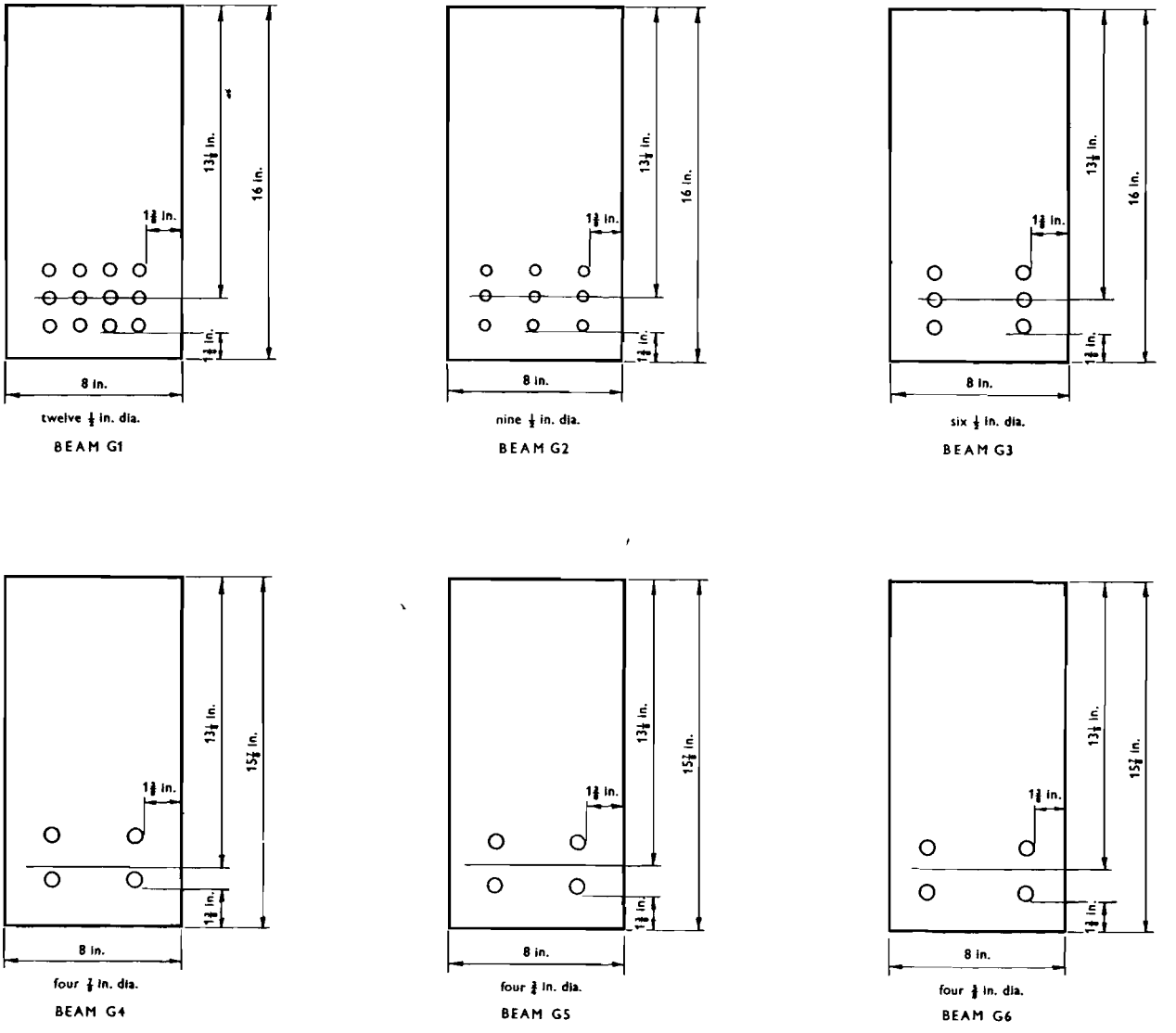

Figure 11: Beams for investigation of percentage reinforcement.

TABLE 2: **Details of the beams in the main investigation.**

Beam No.	Series	Casting	Beam code	Variable within series	Variable between series or casting	Beam dimensions						Reinforcement			Concrete			Remarks
						Depth (in.)	Effect. depth (in.)	Width Comp. (in.)	Width Tens. (in.)	Cover* Bottom (in.)	Cover* Side (in.)	Type	Size **	%	Cube strength (lb/in²)	Indirect tensile strength (lb/in²)	Modulus of rupture (lb/in²)	
1	A1	1	A1M1	Type of bar	Size of bar compared in A1, A2, A3	15⅛	13⅛	8	8	1⅜	1⅜	Mild steel	2 No. 10	2·33	5,320	445	454	
2			A1S1			15⅛	13⅛	8	8	1⅜	1⅜	Sq. twisted	2 No. 10	2·33	5,050	445	454	
3			A1H1			15⅛	13⅛	8	8	1⅜	1⅜	Helibond	2 No. 10	2·33	5,400	445	454	
4			A1U1			15⅛	13⅛	8	8	1⅜	1⅜	Unisteel 60	2 No. 10	2·33	5,350	445	454	
5			A1U2			15⅛	13⅛	8	8	1⅜	1⅜	Unisteel 60	2 No. 10	2·33	4,980	445	454	
6			A1W1			15⅛	13⅛	8	8	1⅜	1⅜	Welbond 60	2 No. 10	2·33	5,180	445	454	
7		2	A1M3	Type of bar		15⅛	13⅛	8	8	1⅜	1⅜	Mild steel	2 No. 10	2·33	4,600	414	420	
8			A1S3			15⅛	13⅛	8	8	1⅜	1⅜	Sq. twisted	2 No. 10	2·33	4,580	414	420	
9			A1H3			15⅛	13⅛	8	8	1⅜	1⅜	Helibond	2 No. 10	2·33	4,500	414	420	
10			A1U3			15⅛	13⅛	8	8	1⅜	1⅜	Unisteel 60	2 No. 10	2·33	4,520	414	420	
11			A1U4			15⅛	13⅛	8	8	1⅜	1⅜	Unisteel 60	2 No. 10	2·33	4,550	414	420	
12			A1W3			15⅛	13⅛	8	8	1⅜	1⅜	Welbond 60	2 No. 10	2·33	4,600	414	420	
13	A2	1	A2M1	Type of bar		15¾	13⅛	8	8	1⅜	1⅜	Mild steel	4 No. 7	2·29	4,940	424	454	
14			A2S1			15¾	13⅛	8	8	1⅜	1⅜	Sq. twisted	4 No. 7	2·29	4,840	424	454	
15			A2H1			15¾	13⅛	8	8	1⅜	1⅜	Helibond	4 No. 7	2·29	4,910	424	454	
16			A2U1			15¾	13⅛	8	8	1⅜	1⅜	Unisteel 60	4 No. 7	2·29	4,810	424	454	
17			A2W1			15¾	13⅛	8	8	1⅜	1⅜	Welbond 60	4 No. 7	2·29	4,940	424	454	
18			A2W2			15¾	13⅛	8	8	1⅜	1⅜	Welbond 60	4 No. 7	2·29	4,880	424	454	
19		2	A2M3	Type of bar		15¾	13⅛	8	8	1⅜	1⅜	Mild steel	4 No. 7	2·29	4,910	356	415	
20			A2S3			15¾	13⅛	8	8	1⅜	1⅜	Sq. twisted	4 No. 7	2·29	4,910	356	415	
21			A2H3			15¾	13⅛	8	8	1⅜	1⅜	Helibond	4 No. 7	2·29	4,780	356	415	
22			A2U3			15¾	13⅛	8	8	1⅜	1⅜	Unisteel 60	4 No. 7	2·29	4,750	356	415	
23			A2W3			15¾	13⅛	8	8	1⅜	1⅜	Welbond 60	4 No. 7	2·29	4,870	356	415	
24			A2W4			15¾	13⅛	8	8	1⅜	1⅜	Welbond 60	4 No. 7	2·29	4,830	356	415	
25	A3	1	A3M1	Type of bar		16	13⅛	8	8	1⅜	1⅜	Mild steel	12 No. 4	2·24	4,440	342	433	
26			A3S1			16	13⅛	8	8	1⅜	1⅜	Sq. twisted	12 No. 4	2·24	4,380	342	433	
27			A3H1			16	13⅛	8	8	1⅜	1⅜	Helibond	12 No. 4	2·24	4,410	342	433	
28			A3U1			16	13⅛	8	8	1⅜	1⅜	Unisteel 60	12 No. 4	2·24	4,300	342	433	
29			A3W1			16	13⅛	8	8	1⅜	1⅜	Welbond 60	12 No. 4	2·24	4,340	342	433	
30			A3W2			16	13⅛	8	8	1⅜	1⅜	Welbond 60	12 No. 4	2·24	4,440	342	433	Actual bottom cover ½ in.
31		2	A3M3	Type of bar		16	13⅛	8	8	1⅜	1⅜	Mild steel	12 No. 4	2·24	5,620	—	476	
32			A3S3			16	13⅛	8	8	1⅜	1⅜	Sq. twisted	12 No. 4	2·24	5,490	—	476	
33			A3H3			16	13⅛	8	8	1⅜	1⅜	Helibond	12 No. 4	2·24	5,540	—	476	
34			A3U3			16	13⅛	8	8	1⅜	1⅜	Unisteel 60	12 No. 4	2·24	5,450	—	476	
35			A3W3			16	13⅛	8	8	1⅜	1⅜	Welbond 60	12 No. 4	2·24	5,580	—	476	
36			A3W4			16	13⅛	8	8	1⅜	1⅜	Welbond 60	12 No. 4	2·24	5,740	—	476	

Beam No.	Series	Casting	Beam code	Variable within series	Variable between series or casting	Beam dimensions						Reinforcement			Concrete			Remarks
						Depth (in.)	Effect. depth (in.)	Width		Cover*		Type	Size **	%	Cube strength (lb/in²)	Indirect tensile strength (lb/in²)	Modulus of rupture (lb/in²)	
								Comp. (in.)	Tens. (in.)	Bottom (in.)	Side (in.)							
37	B	1	B1P1	Cover in beams with stirrups	Bar type compared in two castings	15⅛	13⅛	8	8	1⅜	1⅜	Mild steel	4 No. 7	2·29	3,843	319	392	⅜ in. diameter mild steel stirrups at 6 in. centres in constant bending moment zone
38			B1P2			15⅛	13⅛	8	8	1⅜	1⅜	Mild steel	4 No. 7	2·29	3,843	319	392	
39			B2P1			15¾	13⅛	8	8	¾	¾	Mild steel	4 No. 7	2·29	3,843	319	392	
40			B2P2			15⅜	13⅛	8	8	¾	¾	Mild steel	4 No. 7	2·29	3,843	319	392	
41		2	B1D1			15⅛	13⅛	8	8	¾	¾	G.K.60	4 No. 7	2·29	4,175	348	405	
42			B1D2			15⅛	13⅛	8	8	¾	¾	G.K.60	4 No. 7	2·29	4,190	348	405	
43			B2D1			15¾	13⅛	8	8	1⅜	1⅜	G.K.60	4 No. 7	2·29	4,203	348	405	
44			B2D2			15¾	13⅛	8	8	1⅜	1⅜	G.K.60	4 No. 7	2·29	4,216	348	405	
45	C	1	C1P	Side cover and beam width	Bar type compared in two castings	15¾	13⅛	8	3½	1⅜	½	H.T. round	4 No. 7		4,820	352	421	T beam
46			C2P			15¾	13⅛	8	5½	1⅜	1½	H.T. round	4 No. 7		4,870	352	421	T beam
47			C3P			15¾	13⅛	8	7⅜	1⅜	2⅝	H.T. round	4 No. 7		4,900	352	421	T beam
48			C4P			16	13⅜	6¼	6¼	1⅜	½	Mild steel	12 No. 4	2·67	4,320	352	421	
49			C5P			16	13⅜	8	8	1⅜	1⅜	Mild steel	12 No. 4	2·25	4,550	352	421	
50			C6P			16	13⅛	9¾	9¾	1⅜	2¼	Mild steel	12 No. 4	1·84	4,500	352	421	
51		2	C1D			15¾	13⅛	8	3½	1⅜	½	G.K.60	4 No. 7		5,270	472	477	T beam
52			C2D			15¾	13⅛	8	5½	1⅜	1½	G.K.60	4 No. 7		5,320	472	477	T beam
53			C3D			15¾	13⅛	8	7¾	1⅜	2⅝	G.K.60	4 No. 7		5,050	472	477	T beam
54			C4D			16	13⅜	6¼	6¼	1⅜	½	G.K.60	12 No. 4	2·67	5,210	472	477	
55			C5D			16	13⅜	8	8	1⅜	1⅜	G.K.60	12 No. 4	2·25	5,300	472	477	
56			C6D			16	13⅛	9¾	9¾	1⅜	2¼	G.K.60	12 No. 4	1·84	5,340	472	477	
57	D	1	D1	Bottom cover		17⅛	13⅛	8	8	2¾	1⅜	G.K.60	4 No. 7	2·29	3,800	—	396	
58			D2			17⅛	13⅛	8	8	2¾	1⅜	G.K.60	4 No. 7	2·29	3,880	—	396	
59			D3			16⅛	13⅛	8	8	1¾	1⅜	G.K.60	4 No. 7	2·29	3,950	—	396	
60			D4			16⅛	13⅛	8	8	1¾	1⅜	G.K.60	4 No. 7	2·29	4,000	—	396	
61			D5			14⅞	13⅛	8	8	½	1⅜	G.K.60	4 No. 7	2·29	4,190	—	396	
62			D6			14⅞	13⅛	8	8	½	1⅜	G.K.60	4 No. 7	2·29	4,240	—	396	
63	E	1	E1P	Layout of bars and bar type		14⅞	13⅛	8	8	½	11/16	H.T. round	4 No. 7	2·29	4,600	374	419	
64			E2P			15⅜	13⅛	8	8	1⅜	1 9/16	H.T. round	4 No. 7	2·29	4,800	374	419	
65			E3P			15⅜	13⅛	8	8	1⅝	3¼	H.T. round	4 No. 7	2·29	4,850	374	419	
66			E1D			14⅞	13⅛	8	8	½	11/16	G.K.60	4 No. 7	2·29	4,700	374	419	
67			E2D			15⅜	13⅛	8	8	1⅜	1 9/16	G.K.60	4 No. 7	2·29	4,950	374	419	
68			E3D			15¾	13⅛	8	8	1⅝	3¼	G.K.60	4 No. 7	2·29	5,160	374	419	
69	F	1	F1	Concrete strength		15¾	13⅛	8	8	1⅜	1⅜	G.K.60	4 No. 7	2·29	2,950	294	350	Tested at 14 days
70			F2			15¾	13⅛	8	8	1⅜	1⅜	G.K.60	4 No. 7	2·29	2,985	248	340	Compaction factor 0·92
71			F3			15¾	13⅛	8	8	1⅜	1⅜	G.K.60	4 No. 7	2·29	4,960	389	425	Compaction factor 0·88
72			F4			15¾	13⅛	8	8	1⅜	1⅜	G.K.60	4 No. 7	2·29	2,827	247	360	Compaction factor 0·95
73			F5			15¾	13⅛	8	8	1⅜	1⅜	G.K.60	4 No. 7	2·29	3,475	—	—	Tested at 35 days
74			F6			15¾	13⅛	8	8	1⅜	1⅜	G.K.60	4 No. 7	2·29	4,900	—	510	Tested at 85 days

TABLE 2 *continued*

Beam No.	Series	Casting	Beam code	Variable within series	Variable between series or casting	Beam dimensions						Reinforcement			Concrete			Remarks
						Depth (in.)	Effect. depth (in.)	Width		Cover*		Type	Size **	%	Cube strength (lb/in²)	Indirect tensile strength (lb/in²)	Modulus of rupture (lb/in²)	
								Comp. (in.)	Tens. (in.)	Bottom (in.)	Side (in.)							
75	G	1	G1P	Steel % and bar diameter	Bar type	16	13⅛	8	8	1⅜	1⅜	Mild steel	12 No. 4	2·25	4,770	365	515	
76			G2P			16	13⅛	8	8	1⅜	1⅜	Mild steel	9 No. 4	1·68	4,980	365	515	
77			G3P			16	13⅛	8	8	1⅜	1⅜	Mild steel	6 No. 4	1·12	5,050	365	515	
78			G4P			15¾	13⅛	8	8	1⅜	1⅜	Mild steel	4 No. 7	2·29	4,700	365	515	
79			G5P			15¾	13⅛	8	8	1⅜	1⅜	Mild steel	4 No. 6	1·68	4,500	365	515	
80			G6P			15¾	13⅛	8	8	1⅜	1⅜	Mild steel	4 No. 5	1·17	4,940	365	515	
81		2	G1D			16	13⅛	8	8	1⅜	1⅜	G.K.60	12 No. 4	2·25	4,850	375	415	
82			G2D			16	13⅛	8	8	1⅜	1⅜	G.K.60	9 No. 4	1·68	4,775	375	415	
83			G3D			16	13⅛	8	8	1⅜	1⅜	G.K.60	6 No. 4	1·12	5,020	375	415	
84			G4D			15¾	13⅛	8	8	1⅜	1⅜	G.K.60	4 No. 7	2·29	5,190	375	415	
85			G5D			15¾	13⅛	8	8	1⅜	1⅜	G.K.60	4 No. 6	1·68	4,960	375	415	
86			G6D			15¾	13⅛	8	8	1⅜	1⅜	G.K.60	4 No. 5	1·17	4,900	375	415	
87		2R	G1DR			16	13⅛	8	8	1⅜	1⅜	G.K.60	12 No. 4	2·25	4,340	326	389	
88			G2DR			16	13⅛	8	8	1⅜	1⅜	G.K.60	9 No. 4	1·68	4,150	326	389	
89			G3DR			16	13⅛	8	8	1⅜	1⅜	G.K.60	6 No. 4	1·12	4,540	326	389	
90	H	1	H1V	Inverted casting		15¾	13⅛	8	8	1⅜	1⅜	G.K.60	4 No. 7	2·29	4,085	—	—	*V* means steel in bottom of mould; *R* in top
91			H1R			15¾	13⅛	8	8	1⅜	1⅜	G.K.60	4 No. 7	2·29	4,048	—	—	
92			H2V			15¾	13⅛	8	8	1⅜	1⅜	G.K.60	4 No. 7	2·29	4,150	—	—	
93			H2R			15¾	13⅛	8	8	1⅜	1⅜	G.K.60	4 No. 7	2·29	4,279	—	—	
94	J	1	J1	Curing		15¾	13⅛	8	8	1⅜	1⅜	Hibond A	4 No. 7	2·29	3,410	252	350	J1 kept wet for 1 month
95			J2			15¾	13⅛	8	8	1⅜	1⅜	Hibond A	4 No. 7	2·29	4,400	354	428	J2 kept damp for 1 week
96			J3			15¾	13⅛	8	8	1⅜	1⅜	Hibond A	4 No. 7	2·29	4,670	358	405	J3 exposed after 1 day
97	K	1	K1	Length of shear span		15¾	13⅛	8	8	1⅜	1⅜	Welbond 60	4 No. 7	2·29	4,360	349	450	
98			K2			15¾	13⅛	8	8	1⅜	1⅜	Welbond 60	4 No. 7	2·29	4,360	349	450	
99			K3			15¾	13⅛	8	8	1⅜	1⅜	Welbond 60	4 No. 7	2·29	4,360	349	450	
100	L	1	L1D	Side cover and beam width		15¾	14	8	3½	1⅜	½	G.K.60	2 No. 7		4,080	347	317	T beams
101			L2D			15¾	14	8	5½	1⅜	1½	G.K.60	2 No. 7		4,060	347	317	T beams
102			L3D			15¾	14	8	7¾	1⅜	2⅝	G.K.60	2 No. 7		3,920	347	317	T beams
103			L4D			16	14⅜	6¼	6¼	1⅜	½	G.K.60	6 No. 4	1·26	4,040	347	317	
104			L5D			16	14⅜	8	8	1⅜	1⅜	G.K.60	6 No. 4	1·03	4,110	347	317	
105			L6D			16	14⅜	9¾	9¾	1⅜	2¼	G.K.60	6 No. 4	0·85	3,940	347	317	

* Nominal cover.

** Diameter or equivalent diameter in ⅛ in.

9: CURING

Three beams were subjected to different curing conditions. All were removed from their formwork after one day. One was then immediately allowed to dry out in the warm laboratory atmosphere, one was covered in polythene sheet for seven days after casting and the other was covered in damp hessian and polythene sheet until two days before testing. Shrinkage specimens treated in the same way as the beams showed shrinkage movements in the ratios 9:5:1.

10: WHETHER THE REINFORCEMENT WAS IN THE TOP OR BOTTOM OF THE SECTION AS CAST

Four beams were cast together, two with the reinforcement in the bottom of the mould and two with the reinforcement in the top.

Details of test programme

Apart from trial beams to determine the suitability of the chosen sections, the programme consisted of 105 beams in the initial investigation and a further 28 beams tested subsequently. The over-all size of the beams was approximately 8 in. wide by 16 in. deep by 17 ft long, and all were tested under symmetrical two-point loading on a 15 ft span. Of the 105 beams, nineteen were reinforced with plain round mild steel, six with plain round high-tensile steel, six with square-twisted steel and 74 with various ribbed high-tensile steels. Of the additional 28 beams, twelve were 'identical' beams containing plain round mild steel reinforcement and twelve were 'identical' beams containing ribbed, high-tensile reinforcement. They were cast in six castings of four beams each, two beams in each casting having plain round reinforcement and two having ribbed reinforcement. The remaining four beams contained a star-section reinforcement.

Reinforcement sizes ranged from $\frac{1}{2}$ in to $1\frac{1}{4}$ in. and steel percentages from 0·85% to 2·67%.

Details of the 105 beams in the initial investigation are given in Table 2 and of the 28 beams in the supplementary investigation in Table 1 of Research Report 18 Part, 2. It can be seen that, in the main investigation, the effect of varying the type of bar was investigated primarily within each of the six castings in Series A1, A2 and A3 (36 beams) but also within Series E (six beams in one casting) and between castings in Series C (twelve beams in two castings).

Direct comparison between plain and ribbed reinforcement was also made in 24 beams of the supplementary series.

The effect of varying bar size was investigated by comparing the results of Series A1, A2 and A3.

The effect of varying cover was investigated primarily in Series C, D, E and L (thirty beams) but also in Series B (eight beams).

The effect of varying reinforcement percentage was investigated primarily with the castings of Series G (fifteen beams) but also by comparison between Series C and Series L.

The remaining parameters were investigated within smaller groups of beams.

Specimen manufacture and control

Beams were cast in groups of up to six and great importance was attached to reducing to a minimum undesired variation between beams in a casting. A group of six beams required twelve batches of concrete which were combined in pairs and then distributed in equal layers in each mould. Poker vibrators were used to compact the concrete, similar treatment being given to each beam. The beams were generally moist cured under polythene sheet for seven days before being transferred together to the laboratory for instrumentation and storage in the laboratory atmosphere until tested at about 21 to 28 days.

The concrete consisted of $\frac{3}{4}$ in. Thames gravel, $\frac{3}{8}$ in. Thames gravel, sand and ordinary Portland cement in the proportions 1·38:2·14:2·10:1 by weight. The water/cement ratio was approximately 0·5 (except in Series F). A compaction factor of 0·91 $\pm$ 0·01 was specified initially but this was increased to 0·93 $\pm$ 0·01 after the first six beams to increase the time taken to reach the desired strength at testing of approximately 4,500 lb/in^2.

Timber moulds, treated to give a smooth finish to the concrete, were used. Except where the effect of casting the beam upside down was being investigated (Series H), the beams were cast with the tension zone at the bottom of the mould. The beams were, however, all tested with the tension zone uppermost to facilitate crack measurement.

Concrete control specimens were made for each pair of batches; generally three 6 in. cubes, one 4 in. by 4 in. by 20 in. beam for flexure testing and one 6 in. by 12 in. cylinder for E tests and the indirect tension test were made. The results were averaged for a group of beams, except in Series F and J, but allowance made in the cube results for the small variation in the age of the beam at testing that was inevitable because each beam took approximately one day to test. Results of tests on control specimens are given in Table 2 and in Research Report 18, Part 2, Table 1.

The condition of the reinforcement was generally 'as milled' but any loose scale or rust that had developed was removed by wire brushing. Typical stress-strain curves for several of the types of steel used are shown in Figure 12.

No stirrups were used in the uniform bending moment zone (generally the central 80 in.) except in those beams in which the influence of stirrups on crack formation was under investigation (Series B). Also, no

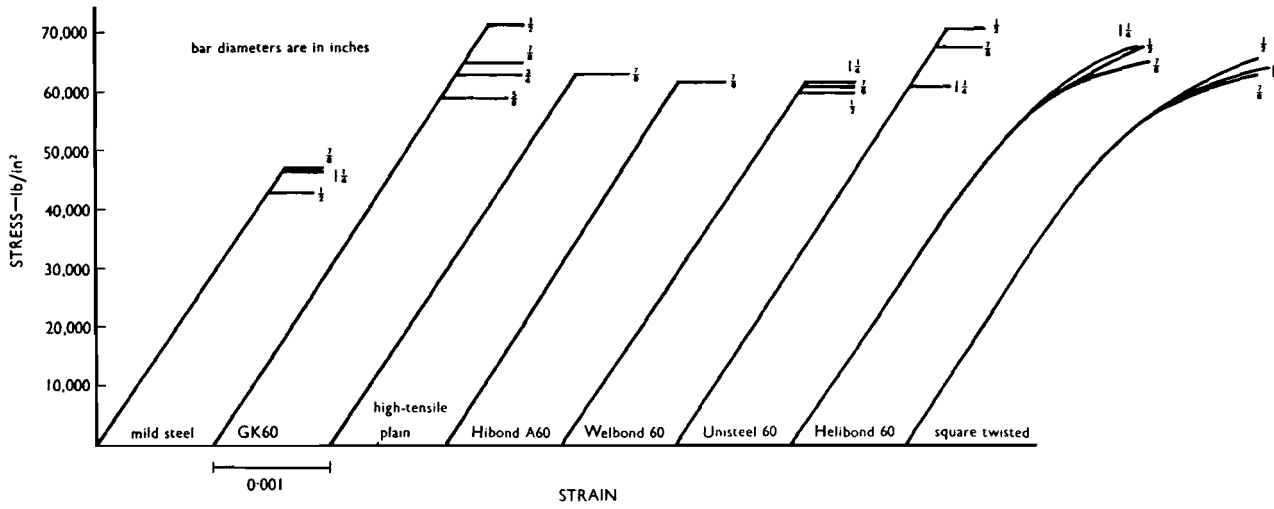

Figure 12: Typical stress-strain curves of reinforcement steels used in the investigation.

permanent spacers were used on the reinforcement in the uniform bending moment zone because it was feared that they might influence cracking. Instead, timber spacers were used and withdrawn as casting proceeded but this did not entirely eliminate variations in cover to the reinforcement. It was therefore necessary, after testing, to expose the reinforcement at important points and measure the cover.

Within the shear spans of the beams $\frac{3}{8}$ in. diameter mild steel stirrups at 4 in. centres were used, together with plastic bar positioners.

Test procedure

All the beams, except those used for the investigation of the effect of shear span, were tested on a 180 in. span and loaded symmetrically at two points to give an 80 in. long zone of uniform bending. All the beams were tested with the tension face uppermost to facilitate crack measurement.

Each crack was measured, with microscopes with a magnification of 25 and calibrated in 0·001 in. divisions, at nine positions at every load stage; the nine positions were: both edges, the centre-line of the tension face, and $1\frac{1}{2}$, 3 and $4\frac{1}{2}$ in. from the tension face down each side of the beam. In a typical test about 1,500 measurements of crack width were made. Each measurement was entered on a specially prepared form (Figure 13) giving the position of the crack and its width at each load stage. After each test the cracks were outlined in ink and photographed.

Strains were measured on the surface of the beams with 8 in. gauge length Demec gauges at three levels along the sides of the beam, namely at the level of the centroid of the reinforcement and at $\frac{1}{2}$ in. and 3 in. from the compression face. On one face there were 24 locating discs at 4 in. centres at each level (giving 22 overlapping gauge lengths covering the whole uniform bending zone) and on the other face there were only two gauge lengths at each level.

In early tests, strains were also measured on the reinforcement but these were later omitted because it was feared that the gauges would influence crack formation and, furthermore, the measurements of strain on the concrete gave adequate information.

Deflexions were measured relative to the supports with dial gauges (0·001 in. divisions) at mid-span and at the loading points. The slope of the beam was measured at fourteen stations along the upper (tension) face by demountable inclinometers.

The general layout of the test rig is shown in Figure 14. The ends of the beams were anchored to the floor by crossheads and pairs of $1\frac{1}{2}$ in. diameter rods which were flexible enough to permit longitudinal freedom. Roller pivots permitted rotational freedom. Load was applied upwards at positions 40 in. on each side of mid-span by 50 ton capacity hand-operated hydraulic jacks. Steel plates and thick rubber pads were incorporated between the jacks and beam to transmit the load and permit the required longitudinal and rotational freedom as deformation occurred. Load was measured by calibrated hydraulic capsules placed under the jacks.

Load was applied to the beams in about six or seven increments until failure occurred.

Method of reduction of data

1: CRACK MEASUREMENT

Every crack visible on the surface of the concrete was measured at, or as near as possible to, the nine grid lines at every load stage and all measurements are included in the analysis of results.

Comparison between the assessments, made by various operators, of a set of cracks was made in the

Crack widths in 0·001 in. units

Beam No. A1H1

Sheet No. 1

Date 21-5-64

POSITION OF CRACK	Load stage 1									2										3										4										5										6										7									
	a	b	c	d	e	f	g	h	j	a	b	c	d	e	f	g	h	j	a	b	c	d	e	f	g	h	j	a	b	c	d	e	f	g	h	j	a	b	c	d	e	f	g	h	j	a	b	c	d	e	f	g	h	j	a	b	c	d	e	f	g	h	j
50 +																																																															
52 +																																																															
54 +																																																															
56 +																																																															
58 +																																																															
60 + ½										2	½	½	½	1	0	½	0	0	4	4	4	3	1	1	3	1	½	5	5	5	5	4	1	3	3	2	5	6	5	4	4	3	4	4	3	6	7	8	6	5	3	5	3	3	11	9	6	7	5	3	6	4	4
62 + 1																																																															
64 +																																																															
66 + 1¼										1	½	1	1	1	0	½	½	0	½	3	3	2	2	2	1	2	1½	5	5	6	6	3	3	3	3	2	7	5	5	6	6	6	3	4	3	7	7	10	9	5	7	5	4	4	8	9	6	12	6	5	6	4	4
68 + 1¼																			0	½	0	0	0	0	0	0	0	0	2	2	0	0	0	½	0	0	0	4	2	0	0	0	½	0	0	½	5	13	0	0	0	2	0	0	2	6	6	0	0	0	4	2	0
70 +																																																															
72 +																																																															
74 + ¼										2	1	2	0	0	0	1	½	½	3	3	4	3	1	1½	3	2	2	6	6	5	4	1	3	1	3	2	6	7	6	4	4	3	5	2½	3	9	9	8	6	4	6	6	4	4	13	14	9	11	6	7	8	4	4
76 +																																																															
78 + 1½										1	1	1	0	0	0	½	0	0	4	4	3	3	2	2	2	1½	1	5	5	4	5	5	3	4	2	1	6	7	5	7	5	4	4	3	2	8	8	7	7	7	6	5	4	3	11	11	6	6	9	7	7	5	3
80 +																																																															
82 + 1¾																												2	2	2	0	0	0	1	1	½	2	3	2	3	2	1	2	2½	2	4	3	3	3	2	2	3	3	2	6	6	5	5	3	3	4	4	2
84 +																																																															
86 + ½										½	½	1	1	½	0	1	½	0	4	3	3	3	3	½	3	1	1	4	2	3	5	3	3	2	2	1	4	4	4	6	5	4	4	3	2	4	5	5	7	7	5	5	4	2	6	6	6	6	8	5	6	4	3
88 +																																																															
90 +																																																															
92 + 0										1	1	1	½	0	0	½	0	0	4	3	3	2	1	1	1	1½	1	5	5	5	1½	3	1	3	2	2	5	6	6	3	4	4	2	3	2	10	8	8	6	6	6	7	3	3	13	12	14	7	8	7	8	6	3
94 + 1																																																															
96 +																																																															
98 + 0										2	2	1	0	0	0	½	½	0	4	3	3	2	1½	2	1½	1	1	6	5	5	4	3	3	3	2	2	7	6	4	5	3	3	3	3	3	9	8	7	7	5	3	5	3	3	16	9	7	11	8	6	5	4	4
100 + 1¾																			3	3	3	2	1½	0	3	1½	0	4	4	5	3	2	1	4	1	1	4	5	4	4	3	2	4	4	2	7	4	7	5	5	3	4	2	2	9	7	8	7	6	4	6	4	2
102 +																																																															
104 + 0																																																																	
106 + 1										½	½	½	½	0	0	½	0	0	4	2	1½	3	3	2	2	1	1	5	4	4	5	3	2	3	2	2	5	4	4	4	4	4	4	3	2	7	6	5	7	6	4	5	3	3	12	8	7	7	6	7	4	3
108 +																																																															
110 + ¾																			1½	1	2	2	1	0	1½	1	1	4	3	3	3	1	1	2	1	1	4	3	3	3	2	2	3	2	2	6	4	4	4	3	3	2	2	2	6	7	7	7	3	4	3	4	2
112 +																																																															
114 + ¼										3	2	0	½	0	0	1	1	0	4	3	1	3	3	4	0	0	0	6	6	3	4	4	4	2	1½	1	6	6	4	6	6	4	2	2	1½	6	7	6	6	6	7	2	2	½	11	12	6	8	6	5	4	4	4
116 + 0																			0	0	1½	0	0	0	1	1	½	0	0	1	0	0	0	2	1½	½	0	0	1	0	0	0	1	1½	1	0	0	1	0	0	0	2	½	½	0	0	1	0	0	0	2	2	1
118 + ¾																			1	1	0	0	0	0	0	0	0	3	2	0	1	1	1	0	0	0	4	4	1½	2	3	2	1	1½	1½	7	4	3	4	4	3	1	2	2	9	5	4	4	5	2	2	3	2
120 + 1¼																			0	1	1½	0	0	0	1	½	0	0	½	5	0	0	0	2	1	½	½	1	3	0	0	0	4	1½	1	0	2	4	0	0	0	2	1	½	0	2	4	0	0	0	3	2	1
122 + 1										2	1	1	2	0	0	0	0	0	3	3	2	3	1	1½	1	1½	1	6	3	4	5	3	3	1	1½	1	1	4	3	6	3	3	3	4	2	9	6	7	8	4	5	4	3	2	13	7	9	8	7	8	4	4	3
124 +																																																															
126 + 1¾										1	0	½	0	0	0	0	0	0	3	3	2	2	1	0	1	1	½	5	4	4	4	3	2	3	2	1	6	7	6	6	5	3	4	3	2	8	8	7	8	5	3	5	5	3	12	9	7	9	6	6	6	6	3
128 +																																																															
130 +																																																															
132 + 1										½	1	1	½	½	0	1	½	0	5	3	4	1	2	1½	2	1½	1	5	3	6	5	3	3	4	3	2	7	6	5	2	5	4	4	3	3	8	9	8	7	5	5	5	5	3	12	8	11	4	9	7	7	6	4
134 +																																																															
136 +																																																															
138 + 1¾																			4	3	3	2	2	1	2	3	2	3	4	6	4	3	3	4	3	2	5	5	7	5	4	3	4	5	3	7	6	9	7	7	3	9	8	5	11	6	11	8	8	4	9	6	4
140 +																																																															
142 +																																																															
144 + ¼										1	0	1	1½	1	1	½	0	0	3	2	4	3	2½	1	2	3	1	5	2	4	4	3	2	3	3	2	4	4	5	6	4	3	3	2	2	8	5	8	8	4	2	4	3	2	8	6	11	8	4	2	4	3	3
146 +																																																															
148 +																																																															
150 +																																																															

Figure 13: Crack record sheet.

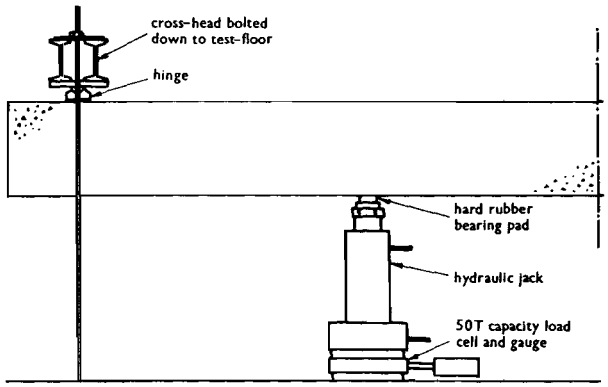

Figure 14: Details of test rig.

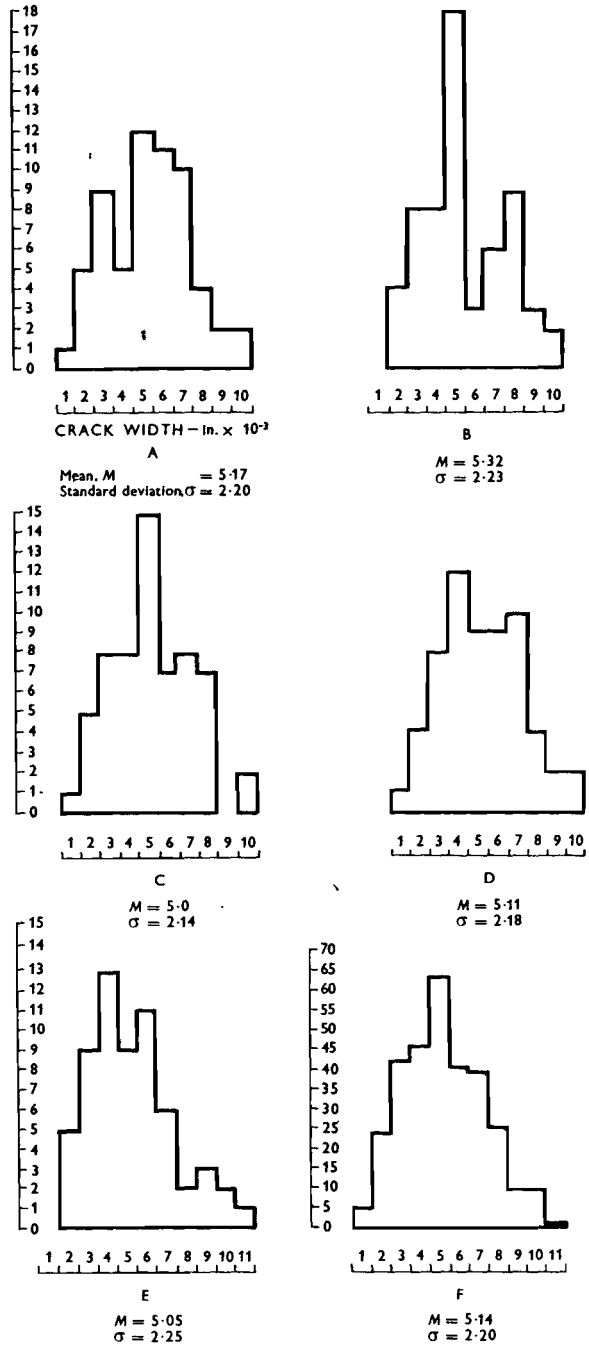

Figure 15: Crack measurement control test (histograms showing comparison of readings taken by different individuals).

early stages of the programme and the histograms and the calculated values of the mean crack widths and standard deviations in Figure 15 show the close agreement between operators.

Measurement of the width of a particular crack at nine positions permitted a profile of the crack width up the sides of the beam to be drawn. Different types of beams had different crack profiles. For beams with approximately equal side and bottom cover to the main reinforcement (and, thus, approximately equal distances from each crack measurement grid line to the nearest reinforcement bar), the width of a crack on the side of the beam was closely proportional to the distance of the point of measurement from the neutral axis of the beam. The average strain of the concrete along the side of a beam (derived from the Demec strain gauge measurements along the entire uniform moment zone) was also proportional to the distance from the neutral axis and therefore plotting the crack width against average concrete strain at the level of the crack measurement gave a straight line for such beams. Since crack width was also proportional to the average steel stress (and thus to the average concrete strain), all measurements of a crack on the sides of a beam, in the linear range of behaviour of the reinforcement, were on a single line as illustrated in Figure 16.

For beams in which the distances from the crack measurement grid lines to the nearest reinforcement were dissimilar the crack width was not dependent solely on the distance from the neutral axis and the measurements at each grid line produced different lines as illustrated in Figure 17. In fact, Figure 16 is simply a particular case of Figure 17.

In practice, instead of plotting the width of a single crack, the mean width m of all cracks in the uniform moment zone of the beam was plotted. Evidence of normal, or Gaussian, distribution of crack widths in a beam was made in several ways, one of which is illustrated in Figure 18. For beam A2W4 the measurements of crack width were each divided by the average strain in the concrete at the surface of the beam at the same level as the crack measurement. The resulting values of ω/ε were grouped and cumulative frequencies were prepared. These were then converted to percentage cumulative frequencies and plotted on normal probability paper (Figure 18). The straight-line plot indicates normal distribution of the values of ω/ε and, thus, of crack widths.

Further confirmation of normal distribution of crack widths in a beam was made by considering a population of 655 crack width measurements on the first 36 beams tested. For normal distribution, it is to be expected that 2·27% of measured values will exceed the value of $(m + 2\sigma)$ for the population. Thus, for the 655 cracks, 14·8 would be expected to be greater than the $(m + 2\sigma)$; in fact 12 measured cracks were greater. The value $(m + 2\sigma)$ is, in fact, a useful approximation to the maximum crack width to be

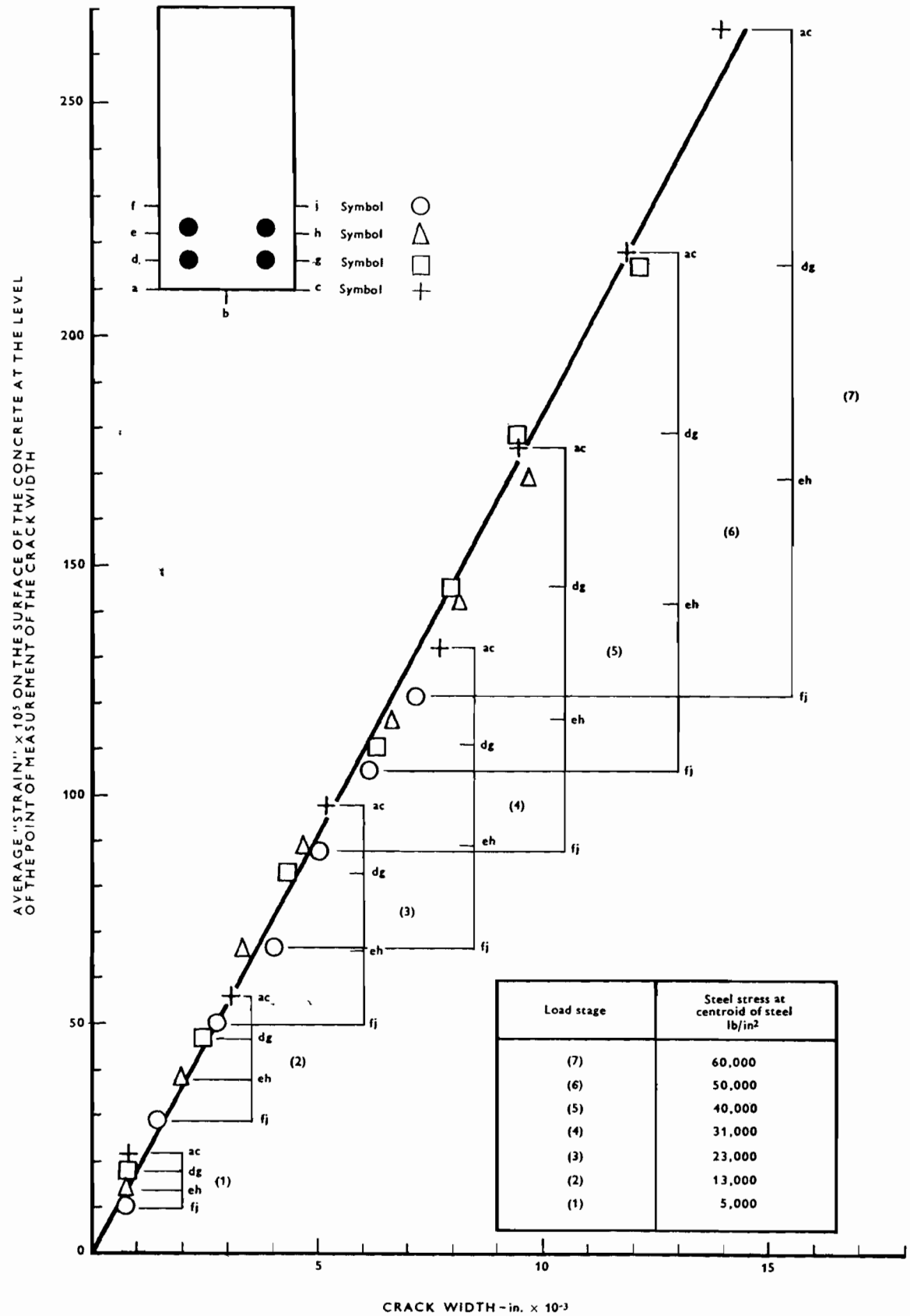

Figure 16: Method of plotting crack width measurements—beam with similar side and bottom cover to reinforcement.

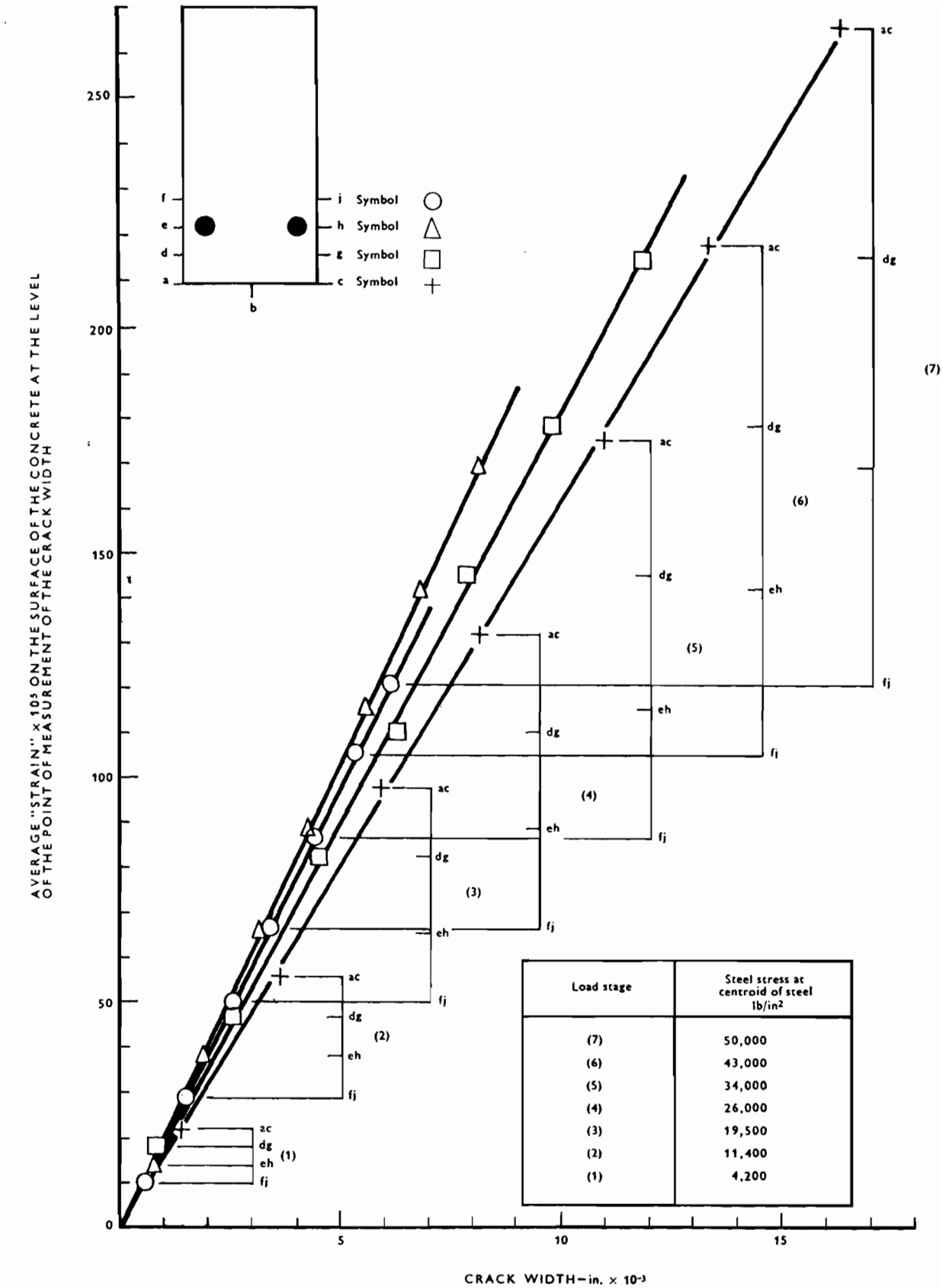

Figure 17: Method of plotting crack width measurements—beam with unequal side and bottom cover.

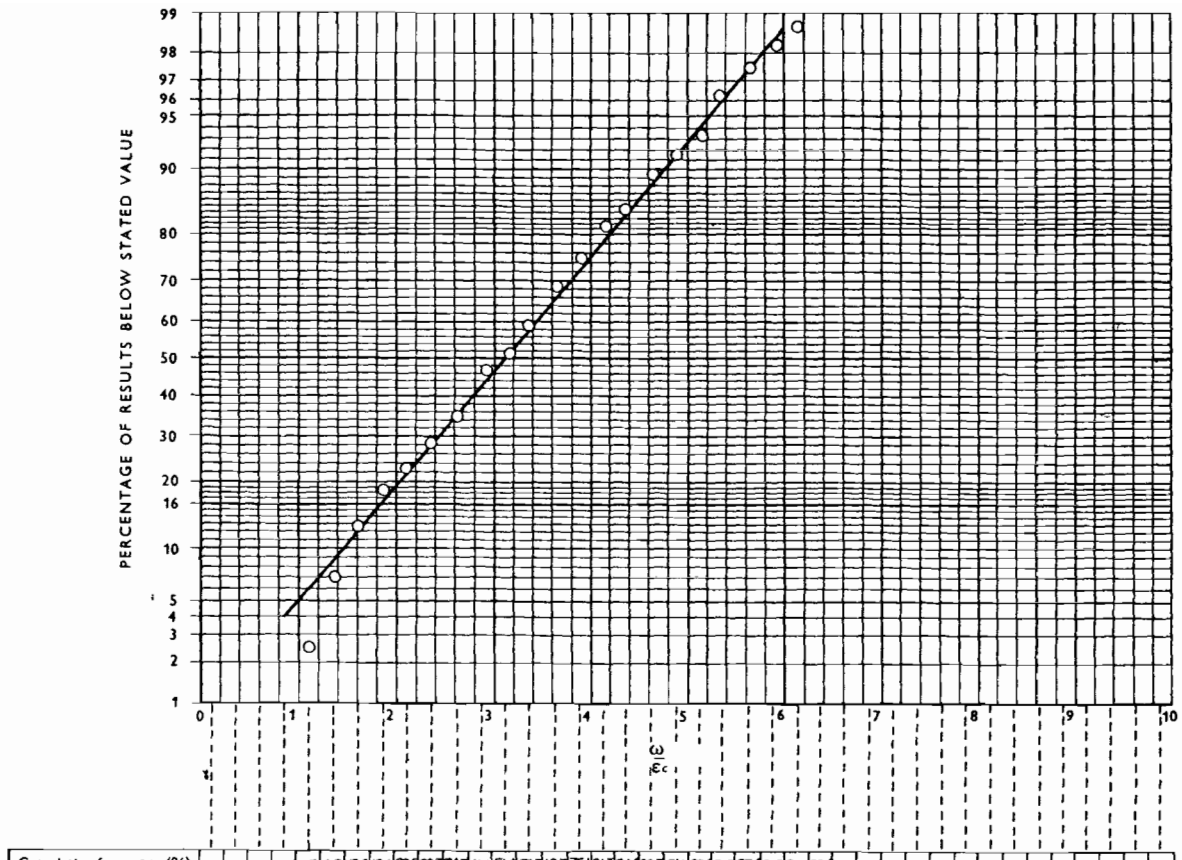

Group intervals (in. x 10^{-3})	Frequency distribution	Frequency	Cumulative frequency	Cumulative frequency (%)
below 125		2	2	0.2
125–375		5	7	0.75
375–625		17	24	2.5
625–875		40	64	6.8
875–1,125		54	118	12.5
1,125–1,375		57	175	18.6
1,375–1,625		38	213	22.5
1,625–1,875		54	267	28.3
1,875–2,125		61	328	34.7
2,125–2,375		111	439	46.6
2,375–2,625		46	485	51.5
2,625–2,875		75	560	59.3
2,875–3,125		89	649	68.7
3,125–3,375		60	709	75.1
3,375–3,625		57	766	81.3
3,625–3,875		31	797	84.4
3,875–4,125		46	843	89.3
4,125–4,375		24	867	91.6
4,375–4,625		14	881	93.4
4,625–4,875		28	909	96.3
4,875–5,125		10	919	97.4
5,125–5,375		7	926	98.2
5,375–5,625		5	931	98.7
5,625–5,875		7	938	99.4
5,875–6,125		4	942	99.8
6,125–6,375		1	943	99.9
6,375–6,625		1	944	100
6,625–6,875				
6,875–7,125				
7,125–7,375				
7,375–7,625				
7,625–7,875				
7,875–8,125				
8,125–8,375				
8,375–8,625				
8,625–8,875				
8,875–9,125				
9,125–9,375				
9,375–9,625				
9,625–9,875				

Figure 18: Demonstration of Gaussian distribution of crack widths.

expected in practice. Being derived from measurements on the entire population of cracks in a beam it is subject to less experimental error than the measured value of maximum crack width in the beam. In many of the graphs in this report the values of both $(m + 2\sigma)$ and mean crack width have been plotted for the various measurement grid lines.

Although the stress in the reinforcement is not used directly as one of the axes in this method of plotting, the steel stress may be calculated by reading off the strain in the concrete at the level of the reinforcement, at each load stage, and multiplying by the modulus of elasticity of the steel. (The average steel strain is equal to the average concrete strain at the same level.) This has been done in the explanatory graphs of Figures 16 and 17 but has not been done in the graphs of the actual results in the report.

The basis used in this report for comparison of crack widths in various beams is comparison of the slopes of lines such as those in Figures 16 and 17. By this method all measurements are included in the analysis; some 150,000 measurements of crack width were made in the initial investigation. The lines plotted were, in all cases, computed best-fit lines for the results.

The calculations of mean crack widths and standard deviations for each beam were made using a Sirius digital computer; the following values were calculated and tabulated at each load stage.

(a) The mean crack width, the standard deviation of the crack widths and the number of cracks along each of the nine measurement grid lines.

(b) The mean, standard deviation and number of cracks for the pairs of grid lines on opposite faces of the beam, i.e. for grid lines *a* and *c* (tension face), *d* and *g* (1½ in. down), *e* and *h* (3 in. down) and *f* and *j* (4½ in. down).

(c) The value $\alpha = \sqrt[3]{\frac{\Sigma(m-\omega)^3}{N}}$, which gives a measure of the skewness of the crack width distribution, for the combined measurements on the tension face.

(d) The actual measured maximum width of crack at each load stage.

Values of α were small for all beams, showing symmetrical distribution of crack widths about the mean values.

2: STRAIN MEASUREMENTS

The measurements obtained with Demec mechanical gauges along the constant moment zone at three levels were transferred to punched tape and the computer was used to calculate the neutral axis of the beam and the 'average strain' in the concrete at the level of each crack measurement grid line at each load stage. The 'average strain' so obtained was, in the tension zone, the sum of all the crack widths and the strain in the uncracked concrete. At the level of the reinforcement the 'average strain' in the concrete was, obviously, the same as the average strain in the steel.

The strain measurements with e.r.s. gauges on the reinforcing bars in the early tests gave fair agreement with the Demec readings but were less useful than the Demec readings since they only measured local strain. Furthermore, the e.r.s. gauges acted as crack inducers and were eliminated in the majority of tests.

3: DEFLEXION MEASUREMENTS AND INCLINOMETER MEASUREMENTS

These measurements were used only as a simple comparison between beams in cases where anomalies existed in the results of other forms of observation.

Methods of analysis of results

Although the tests were not planned with the idea of statistical analysis of the effects of the parameters investigated, it became clear that, since the differences between nominally identical beams were of the same order as the differences attributable to some of the main parameters in the programme, a statistical approach to the analysis of the results was very desirable. Thus the results have been considered in two ways: from what may be termed the 'engineering judgement' approach and, so far as is possible, from a statistical approach.

Both methods of analysis were based on the slopes of the graphs of mean crack width *m* and maximum crack width (in fact, $m + 2\sigma$) against the average strain on the surface of the concrete at the level of the crack width measurement.

The 'engineering judgement' analysis consisted of direct comparisons between the slopes of the graphs for particular beams or groups of beams. This was done in tabular form to show the apparent effects of the parameters investigated.

The statistical analysis was based on Student's '*t*' tests. This uses the mean standard deviation and number of observations to determine whether two sets of observations are drawn from the same total population. It is postulated that there is no significant difference between the means of the two populations being compared unless the probability of difference occurring due to chance alone is less than an certain predetermined value. Student's '*t*' is a measure of the probability of the difference occurring due to chance alone and a value of '*t*' corresponding to a 5% probability (for a given number of degrees of freedom) is frequently used as the limit above which the difference between the two means must be considered as being 'probably significant'. Values of '*t*' above that corresponding to a 1% probability would indicate that the difference between the two means is 'highly significant'—that is, unlikely to be due to chance alone.

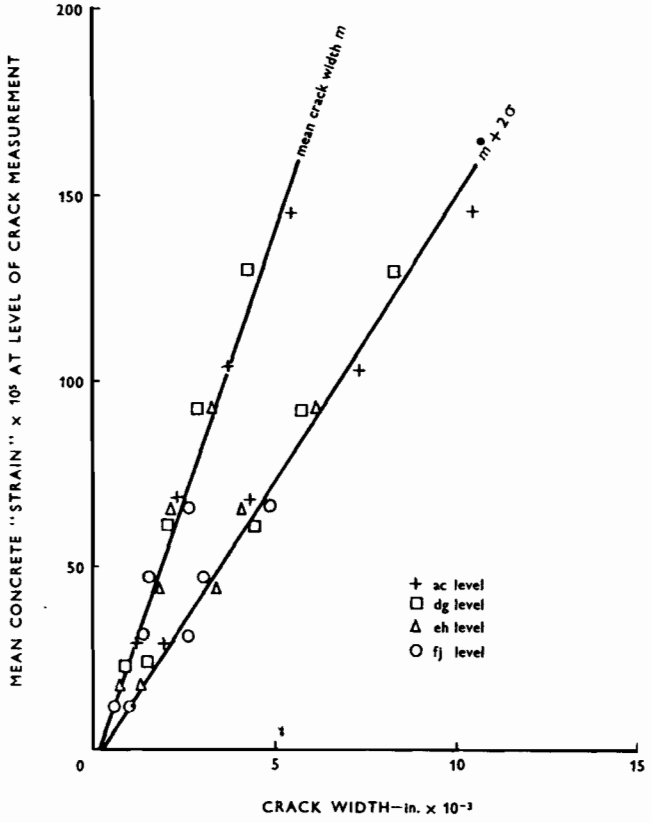

Figure 19: Typical graph of strain against crack width, beam A1M1.

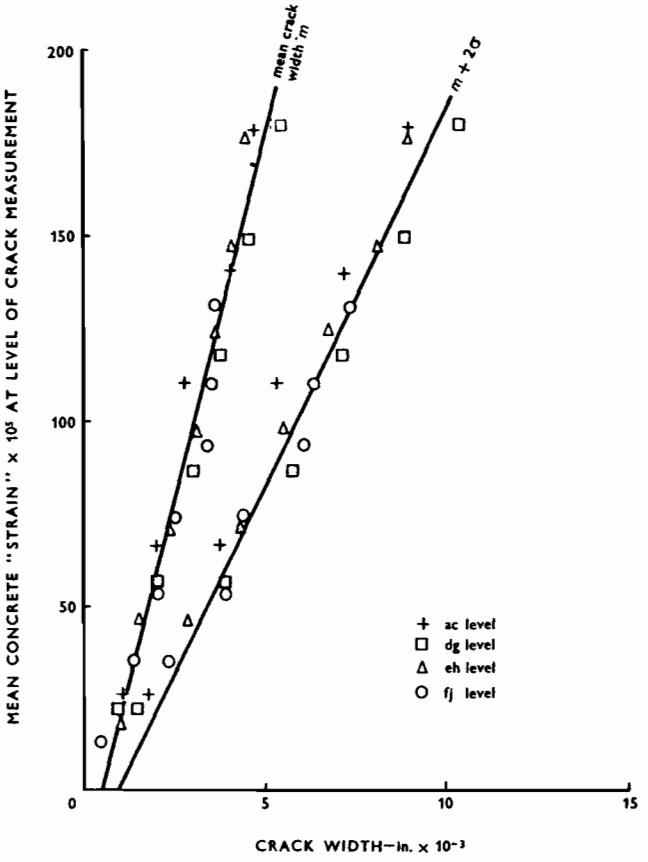

Figure 20: Typical graph of strain against crack width, beam A3H3.

Before the '*t*' tests were carried out, variance ratio tests were made to determine whether the sample variances were sufficiently alike to warrant the assumption that they were independent estimates of the same population; this test was passed in practically all cases.

Results

The effects of the various parameters are, so far as is possible, first discussed separately and then general points arising from the tests are discussed.

1: INFLUENCE OF STEEL STRESS

For stresses within the linear range of behaviour of the steels, it was found that mean crack width and maximum crack width were both closely proportional to the stress in the reinforcement. At very low levels of stress there was a transition from the apparently uncracked beam to the cracked beam but this was a very short zone in most of the beams tested and straight line graphs of crack width against average concrete strain generally passed through, or very close to, the origin.

2: INFLUENCE OF BAR TYPE

The first six castings of six beams each (beams 1–36) were designed particularly to show the influence of bar type on the cracking. In each casting there was one beam with plain round mild steel reinforcement, one with square twisted reinforcement and four with ribbed reinforcement. Superficial comparison of the beams within a group showed no clearly defined influence of bar type; it was, in general, impossible to decide from observation of the crack patterns alone whether a beam contained plain or deformed steel.

It was found that for this group of beams, which had equal side and bottom cover to the reinforcement, plotting crack widths against the average concrete strain at the level of the crack measurement gave a single straight line for all measurements. In Figures 19 and 20 typical graphs* are shown; both the mean crack width and the value $(m + 2\sigma)$ at each of the four measurement levels (*ac, dg, eh, fj*) are plotted for every load stage. Each graph thus represents in excess of 1,000 measurements of crack width.

In Table 3 the slopes of the mean crack line and the $(m + 2\sigma)$ line are tabulated for the 36 beams. The similarity between the majority of beams is noticeable and there are no very clear differences between types of bar. No one type of bar gave consistently poor or

* All of the graphs are reproduced in the Supplement.

consistently good results, the poorest results being obtained with Welbond 60 in one case, Helibond in another, square twisted in a third and mild steel in the remaining three. The best results were obtained with Helibond in two cases, square twisted in two cases, Unisteel 60 in one case and Welbond 60 in one case. (The mean crack slope given in Table 3 is the criterion used.)

In Table 4 various ratios have been calculated for the six castings. The beam with mild steel is compared with the best result with ribbed steel beam, the worst result with ribbed steel, the average result with ribbed steel, the result with square twisted steel and the average result with deformed steel (including square twisted). Ratios for mean crack width and $(m + 2\sigma)$ can be seen to have been very similar to each other while the ratios for $1/N$ values were smaller. The worst and best results for beams with ribbed steel are also compared. The Table indicates that, in general, beams with deformed steel had rather more cracks than those with plain round mild steel and that the cracks were generally smaller for those with deformed steel. The beams with square twisted steel gave results which were, on average, almost identical to the average result for ribbed steel beams and there seems no reason to separate the results of square twisted steel beams from ribbed steel beams.

In some castings the beam with mild steel was better than the worst deformed steel result but in all castings the best deformed steel result was considerably better than the mild steel result. However, the considerable range of results for deformed steel (even between nominally identical beams) precludes the drawing of conclusions regarding relative crack control characteristics of deformed and plain steels.

A statistical investigation of the results of beams 1–36 was made; the following 't' tests were performed.

(1) Each of the four nominally identical beams (Unisteel 60) in Series A1 was compared individually with the total population of four (Table 5).

(2) Each of the four nominally identical beams (Unisteel 60) in Series A1 was compared individually with a total population consisting of the other three (Table 5).

(3, 4) Tests 1 and 2 were repeated with the four nominally identical beams (Welbond 60) in Series A2 (Table 6).

(5, 6) Tests 1 and 2 were repeated with the four nominally identical beams (Welbond 60) in Series A3 (Table 7).

(7) Each of the beams in Series A1 was compared individually with the total population of twelve beams in Series A1 (Table 8).

(8) The combined populations of the nominally identical beams in Series A1 were compared with the total population (Table 8).

TABLE 3: **Summary of results for beams 1–36.**

Beam No.	Reinforcement type*	Number of cracks **	Mean crack slope (in.)	Standard deviation slope (in.)	$\frac{m + 2\sigma}{\varepsilon}$ (in.)
1	MS	37	3·59	1·41	6·41
2	ST	37	3·18	1·43	6·04
3	H	36	2·59	1·14	4·87
4	U	36	3·10	1·16	5·42
5	U	40	3·14	1·39	5·92
6	W	34	3·84	1·29	6·42
7	MS	33	3·53	1·61	6·75
8	ST	40	3·09	1·28	5·65
9	H	34	4·04	1·62	7·28
10	U	42	3·19	1·25	5·69
11	U	34	3·41	1·37	6·15
12	W	38	3·20	1·35	5·90
13	MS	32	4·19	1·72	7·63
14	ST	38	3·05	1·38	5·81
15	H	41	3·46	1·53	6·52
16	U	41	2·61	1·07	4·75
17	W	37	2·77	1·19	5·15
18	W	44	2·82	1·14	5·10
19	MS	34	3·49	1·69	6·87
20	ST	37	3·72	1·65	7·02
21	H	36	3·42	1·46	6·34
22	U	32	3·41	1·20	5·81
23	W	42	2·85	1·15	5·15
24	W	35	2·96	1·21	5·38
25	MS	41	3·40	1·25	5·90
26	ST	45	2·25	1·04	4·33
27	H	44	2·57	1·11	4·79
28	U	48	2·41	1·02	4·45
29	W	46	2·45	1·05	4·55
30	W	41	2·28	0·97	4·22
31	MS	42	3·11	1·12	5·35
32	ST	43	2·80	1·18	5·16
33	H	45	2·64	1·14	4·92
34	U	42	2·72	1·14	5·00
35	W	42	2·67	1·12	4·91
36	W	43	2·92	1·00	4·92

* MS = Plain round mild steel.
ST = Square twisted.
H = Helibond.
U = Unisteel 60.
W = Welbond 60.

** This is the sum of the numbers of cracks on both sides of the beam.

(9, 10) Tests 7 and 8 were repeated for Series A2 (Table 9).

(11, 12) Tests 7 and 8 were repeated for Series A3 (Table 10).

Tests 1–6 were used to determine the values of 't', and the probability levels, corresponding to groups of nominally identical beams. These values were then used as the criteria in the comparisons in tests 7–12.

Table 11 shows the distribution of results of tests 1–6.

Thus it was postulated that values of 't' less than 2·0 indicated no significant difference between the means, values between 2·0 and 3·3 correspond to a

TABLE 4: **Various ratios derived from the results for beams 1–36.**

Beams		Term compared	Ratios					
			Plain round / Best ribbed result	Plain round / Worst ribbed result	Plain round / Mean ribbed result	Plain round / Square twisted result	Plain round / *Mean deformed result	Worst ribbed result / Best ribbed result
Group	Numbers							
A1-1	1-6	$1/N$	1·08	0·92	0·99	1·00	0·99	1·18
		m	1·39	0·93	1·13	1·13	1·13	1·48
		$m+2\sigma$	1·32	1·00	1·13	1·06	1·12	1·32
A1-2	7-12	$1/N$	1·27	1·03	1·12	1·21	1·14	1·24
		m	1·11	0·87	1·02	1·14	1·04	1·26
		$m+2\sigma$	1·19	0·93	1·08	1·19	1·10	1·28
A2-1	13-18	$1/N$	1·37	1·16	1·28	1·19	1·25	1·19
		m	1·60	1·21	1·43	1·37	1·42	1·33
		$m+2\sigma$	1·60	1·17	1·42	1·31	1·39	1·37
A2-2	19-24	$1/N$	1·24	0·94	1·06	1·09	1·07	1·31
		m	1·22	1·02	1·10	0·94	1·07	1·20
		$m+2\sigma$	1·33	1·08	1·21	0·98	1·16	1·23
A3-1	25-30	$1/N$	1·17	1·00	1·10	1·10	1·10	1·17
		m	1·49	1·32	1·40	1·51	1·42	1·13
		$m+2\sigma$	1·40	1·23	1·31	1·36	1·32	1·13
A3-2	31-36	$1/N$	1·07	1·00	1·02	1·02	1·02	1·07
		m	1·18	1·06	1·14	1·11	1·13	1·11
		$m+2\sigma$	1·09	1·07	1·08	1·04	1·07	1·02
all beams	1-36	$1/N$	1·20	1·01	1·10	1·10	1·10	1·19
		m	1·33	1·07	1·20	1·20	1·20	1·25
		$m+2\sigma$	1·32	1·08	1·20	1·16	1·19	1·22

* Including square twisted steel.

TABLE 5: **Student's 't' test results for the four nominally identical beams in Series A1.**

TEST 1		't' Tests
Beam	Degrees of freedom	't'
A1U1	147	−0·44
A1U2	147	−0·27
A1U3	147	−0·08
A1U4	147	0·77

TEST 2		
Beam	Degrees of freedom	't'
A1U1	117	−0·55
A1U2	117	−0·33
A1U3	117	−0·11
A1U4	117	−0·99

TABLE 6: **Student's 't' test results for the four nominally identical beams in Series A2.**

TEST 3		't' Tests
Beam	Degrees of freedom	't'
A2W1	147	−0·34
A2W2	147	−0·13
A2W3	147	0·00
A2W4	147	0·46

TEST 4		
Beam	Degrees of freedom	't'
A2W1	117	−0·45
A2W2	117	−0·16
A2W3	117	0·00
A2W4	117	0·61

TABLE 7: **Student's 't' test results for the four nominally identical beams in Series A3.**

TEST 5		't' Tests
Beam	Degrees of freedom	't'
A3W1	147	−0·61
A3W2	147	−1·42
A3W3	147	0·41
A3W4	147	1·60

TEST 6		
Beam	Degrees of freedom	't'
A3W1	117	−0·77
A3W2	117	−1·83
A3W3	117	0·54
A3W4	117	2·06

TABLE 8: **Student's 't' test results for all beams in Series A1.**

TEST 7		't' Tests
Beam	Degrees of freedom	't'
A1M1	387	1·02
A1S1	387	−0·53
A1H1	387	−2·80
A1U1	387	−0·84
A1U2	387	−0·68
A1W1	387	1·98
A1M3	387	0·78
A1S3	387	0·88
A1H3	387	2·69
A1U3	387	−0·50
A1U4	387	0·34
A1W3	387	−0·46

TEST 8		
Beam	Degrees of freedom	't'
A1M	417	1·22
A1S	417	−0·98
A1H	417	−0·05
A1W	417	1·66

TABLE 9: **Student's 't' test results for all beams in Series A2.**

TEST 9		't' Tests
Beam	Degrees of freedom	't'
A2M1	387	3·48
A2S1	387	−0·66
A2H1	387	0·84
A2U1	387	−2·32
A2W1	387	−1·71
A2W2	387	−1·53
A2M3	387	0·94
A2S3	387	1·78
A2H3	387	0·70
A2U3	387	0·67
A2W3	387	−1·42
A2W4	387	−1·00

TEST 10		
Beam	Degrees of freedom	't'
A2M	417	2·97
A2S	417	0·74
A2U	417	−1·13
A2H	417	1·05

TABLE 10: **Student's 't' test results for all beams in Series A3.**

TEST 11		't' Tests
Beam	Degrees of freedom	't'
A3M1	387	3·32
A3S1	387	−2·01
A3H1	387	−0·51
A3U1	387	−1·27
A3W1	387	−1·08
A3W2	387	−1·88
A3M3	387	2·00
A3S3	387	0·56
A3H3	387	−0·19
A3U3	387	—
A3W3	387	—
A3W4	387	−1·13

TEST 12		
Beam	Degrees of freedom	't'
A3M	417	3·59
A3S	417	−1·01
A3U	417	−0·77
A3H	417	−0·51

TABLE 11: **Results of Student's 't' tests on groups of nominally identical beams in Series A1, A2 and A3 (summary).**

Probability %	30	20	10	5	2	1	0·1
't' (for 120 degrees of freedom)	1·04	1·29	1·66	1·98	2·36	2·62	3·37
Number of results	–20–	———	3	———	———	1 ———	
						(t = 2·06)	

TABLE 12: **Comparison between the slopes of the mean crack-strain graphs for Series B, C, E and G.**

Series	Plain steel		Deformed steel		Ratio plain deformed
	Beam	Slope	Beam	Slope	
B	37—B1P1	2·8	41—B1D1		
	38—B1P2	2·2	42—B1D2	3·3	0·67
	39—B2P1	3·2	43—B2D1	3·2	1·00
	40—B2P2	3·2	44—B2D2	1·7	1·88
C (Level *ac*)	45—C1P	2·9	51—C1D	2·2	1·32
	46—C2P	3·1	52—C2D	2·8	1·11
	47—C3P	4·8	53—C3D	4·6	1·04
	48—C4P	2·3	54—C4D	1·6	1·44
	49—C5P	2·7	55—C5D	2·4	1·13
	50—C6P	4·5	56—C6D	4·9	0·92
E (Level *ac*)	63—E1P	1·3	66—E1D	1·2	1·08
	64—E2P	3·5	67—E2D	3·2	1·09
	65—E3P	5·7	68—E3D	5·8	0·98
G	75—G1P	3·5	81—G1D	3·5	1·00
	76—G2P	2·6	82—G2D	3·1	0·84
	77—G3P	4·4	83—G3D	2·8	1·57
	78—G4P	2·7	84—G4D	2·3	1·17
	79—G5P	3·5	85—G5D	3·1	1·13
	80—G6P	3·1	86—G6D	3·2	0·97
				Mean ratio	1·13

zone of uncertainty and values above 3·3 indicate a real difference between the beams being compared.

Test 7 (Series A1) produced ten values of 't' below 2·0 and only the two Helibond beams gave values of 't' greater than 2·0, both in the zone of uncertainty. Both mild steel beams gave values of 't' less than that for the 30% probability level.

Test 8 (Series A1) produced four values of 't', all less than 2·0. The value for the pair of Helibond beams was extremely small; this result considered in conjunction with test 7 shows that one of the Helibond beams had a good crack control and one a poor crack control but, on average, the Helibond beams were not significantly different from the other types of beam.

In test 9 (Series A2) one beam with mild steel had a 't' of 3·47, i.e. the beam must be considered as different from the remainder but the other beam with mild steel had a 't' of only 0·94. One other value of 't' greater than 2 (2·32) occurred, for a Unisteel beam, placing it in the zone of uncertainty; all other beams had values of 't' less than 2·0.

In test 10 (Series A2) pairing the two beams with mild steel gave a 't' of 2·97 which is in the zone of uncertainty. The other three results were less than 2·0.

In test 11 (Series A3) one of the beams with mild steel was just in the zone of uncertainty and the other was just in the zone of difference. One of the square twisted beams was just in the zone of uncertainty. All the other beams had 't' values less than 2·0.

In test 12 (Series A3) pairing the two beams with mild steel gave a 't' of 3·59, in the zone of difference. All the other beams had 't' values less than 2·0.

Tables 5 to 10 give all the values of 't' for tests 1–12.

Additional 't' tests were carried out on Series A1, A2 and A3, but with the beams with mild steel excluded from the populations. These tests confirmed that there was no significant difference between the results for the various types of deformed steel, including square twisted steel.

Further comparisons between deformed and plain round steel can be made from the results of Series B, C, E and G. In Series B and C the plain and deformed steels were in separate castings and this may have produced differences. In Series E all beams were in one casting but, because of differences in the cover to the reinforcement, crack measurements at each grid line gave different slopes when plotted against strain; only the grid line *ac* (soffit of beam) has been used in the comparisons. Comparison between the slopes of the graphs of mean crack width against strain is given in Table 12; because of other variables comparisons may only be made between pairs of beams. The ratios of the slopes for pairs of beams ranges from 0·67 to 1·88 and have an average value of 1·13, indicating that, on average, the mean crack width was slightly greater for plain round steel than for deformed steel. This result was shown by 't' tests to be 'probably significant'.

The results of the supplementary series of tests comparing twelve beams with mild steel with twelve beams with deformed steel are given in Research Report 18, Part 2.

3: INFLUENCE OF BAR SIZE

The influence of bar size was investigated by comparing Series A1, A2 and A3 containing $1\frac{1}{4}$, $\frac{7}{8}$ and $\frac{1}{2}$ in. bars respectively. The beams with plain round reinforcement were considered separately from the beams with deformed bars. The averages of the mean crack width slopes, of the $(m + 2\sigma)$ slopes and of the number of cracks are given for each series in Table 13. It can be seen that there was no consistent difference between Series A1 and A2 but Series A3 had smaller cracks, and more of them, than the other two series. The difference between Series A3 and Series A1 and A2 was, however, small and (as shown later in the discussion of the influence of cover) was probably caused by the smaller bottom cover that was accidentally used

TABLE 13: **Comparison of beams with various sizes of bar.**

	Mean crack width slope		$(m + 2\sigma)$ slope		Number of cracks (× 2)	
	Plain bars	Deformed bars	Plain bars	Deformed bars	Plain bars	Deformed bars
A1	3·56	3·28	6·58	5·93	35	37
A2	3·84	3·11	7·25	5·70	33	38
A3	3·25	2·57	5·62	4·73	41·5	44

TABLE 14: **Series E, comparison of mean slopes of crack width against strain.**

Beam (plain steel)	Mean crack slope for level			Beam (deformed steel)	Mean crack slope for level		
	ac	*dg*	*eh*		*ac*	*dg*	*eh*
E1P	1·3	0·8	0·8	E1D	1·2	0·9	0·6
E2P	3·5	3·5	2·8	E2D	3·2	2·9	2·4
E3P	5·7	5·8	5·0	E3D	5·8	6·6	5·9

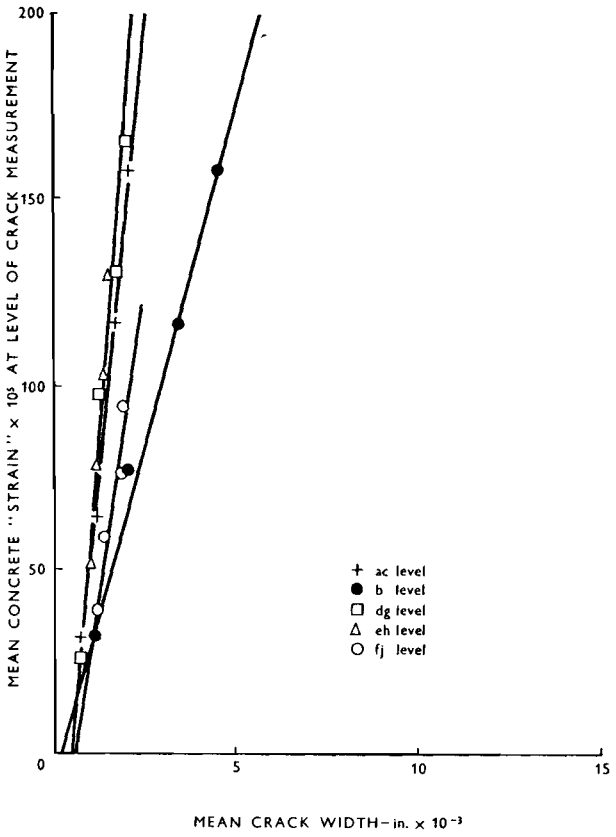

Figure 21: Typical graph of strain against crack width, cover series, beam E1D.

in Series A3. There was certainly no indication of a strong influence of bar size on the crack control characteristics of either plain or deformed steels.

Student's '*t*' tests to compare individual beams in Series A1 with the total population of Series A2 gave no results with values of '*t*' higher than 3·3 and only 2 results between 2·0 and 3·3, indicating that Series A1 and A2 were similar.

Similar comparisons between individual A1 beams and Series A3 gave five results greater than 3·3 and four between 2·0 and 3·3, indicating that Series A1 and A3 were significantly different.

Similarly, comparison between individual beams of Series A2 and Series A3 gave six values of '*t*' greater than 3·3, indicating that Series A2 and A3 were significantly different.

Other '*t*' tests between the total populations of beams with deformed steel in each of Series A1, A2 and A3 gave values of '*t*' indicating similarity between A1 and A2 and a significant difference between A1 and A3 and between A2 and A3.

These '*t*' tests thus confirm the engineering judgement comparisons that Series A1 and A2 were similar to each other but Series A3 was different from Series A1 and from Series A2. These '*t*' tests cannot, of course, show whether the difference was due to varying bar size or to varying cover to the reinforcement.

4: INFLUENCE OF COVER

The effect of varying the cover to the reinforcement was investigated primarily in Series C, D, E and L, totalling thirty beams.

The mean crack width was plotted against the average concrete strain at the level of the crack measurement and, in general, each level produced a separate straight line. Typical graphs are shown in Figures 21 to 23 and all the graphs are shown in the Supplement

In discussing the results it is convenient to deal with Series E first. All the factors which the 'classical' theoretical approach predicts should have an influence on the crack widths were constant within each of two groups of three beams in this series. Thus bar type, bar diameter, steel percentage and the distance of the centroid of the steel from the tension face of the beam were constant and the theory would therefore predict equal crack widths for the three beams. It would, on the other hand, predict a difference between the two groups of 3 beams, one of which used plain round mild steel and the other heavily ribbed steel. In fact, there were very considerable differences within the groups of three but only very small differences between the two groups; this is shown in Table 14.

From the results of Series E it is clear that the 'classical' theory is incapable of predicting even the

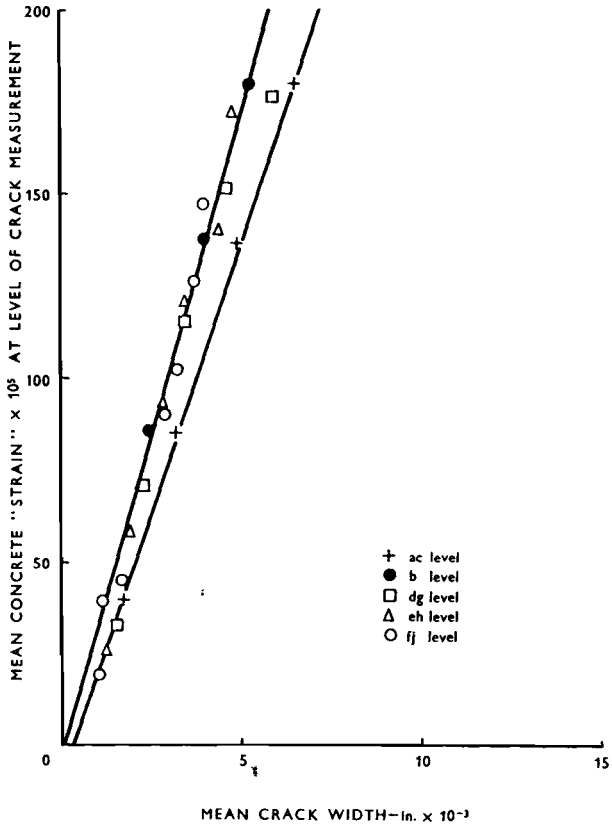

Figure 22: Typical graph of strain against crack width, cover series, beam E2D.

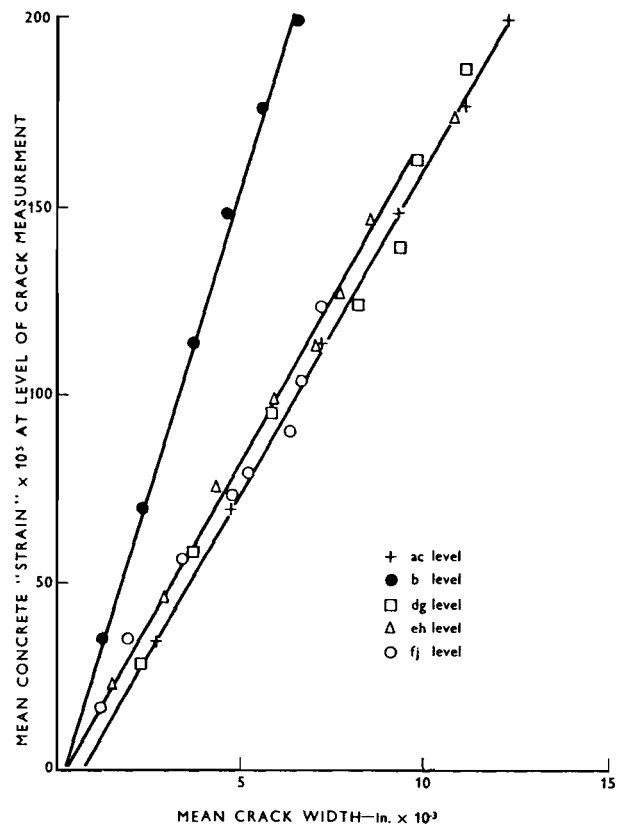

Figure 23: Typical graph of strain against crack width, cover series, beam E3D.

ratios of mean crack widths between various beams and that a completely new basis for predicting crack widths is necessary.

It was found from the results of Series C, D, E and L that, for the range of cover in the tests, the width of a crack was closely proportional to the distance of the point of measurement of the crack from the nearest reinforcing bar.

The results for the thirty beams are plotted in Figures 24 and 25; Figure 24 is for the 21 beams with deformed bars and Figure 25 is for the nine beams with plain bars. Each of the mean crack widths divided by the average concrete strain at the level of the measurement is plotted, except for measurements at level *fj*. In Series L, level *fj* was outside the effective tension zone of the beam and measurements at this level did not follow exactly the same trend as those at other levels; measurements at level *fj* on all beams were therefore omitted from the graphs. Each beam thus, generally, gave four points to be plotted—the averages of *a* and *c*, *d* and *g*, *e* and *h* and the measurement at *b* (centre of soffit)—but where there were appreciable differences in the cover to the reinforcement on the two sides of the beam the measurements at each side were plotted separately. Best-fit lines were computed and drawn through the points. The correlation between crack width and distance to bar is very good and the similarity between the experimental best-fit straight line and the theoretical lines from Figure 6 is evident. The plain steel beam results produced a line slightly above (i.e. indicating wider cracks) that for the deformed steel beams.

In Figures 26 and 27 ultimate mean crack spacings at the various measurement levels have been plotted against the distance to the nearest bar.

As load on a beam was increased the crack spacing approached a limiting value as illustrated for three typical beams in Figure 28. This limiting spacing or 'ultimate mean crack spacing' occurred generally when the average strain in the concrete reached approximately 130×10^{-5}. In Figures 26 and 27 the correlation between the ultimate mean crack spacing and the distance to the nearest bar is very good.

Plain bars appear to give wider spacing than deformed bars at low covers but the lines converge at larger covers. Correlation between the experimental best-fit lines and the theoretical lines in Figure 5 is reasonable.

It is interesting to note that the units of both the crack characteristic ω/ε and the crack spacing are inches and thus the difference between the slopes of the ω/ε graph and the crack spacing graph is a function of true concrete strain. Total extension between the

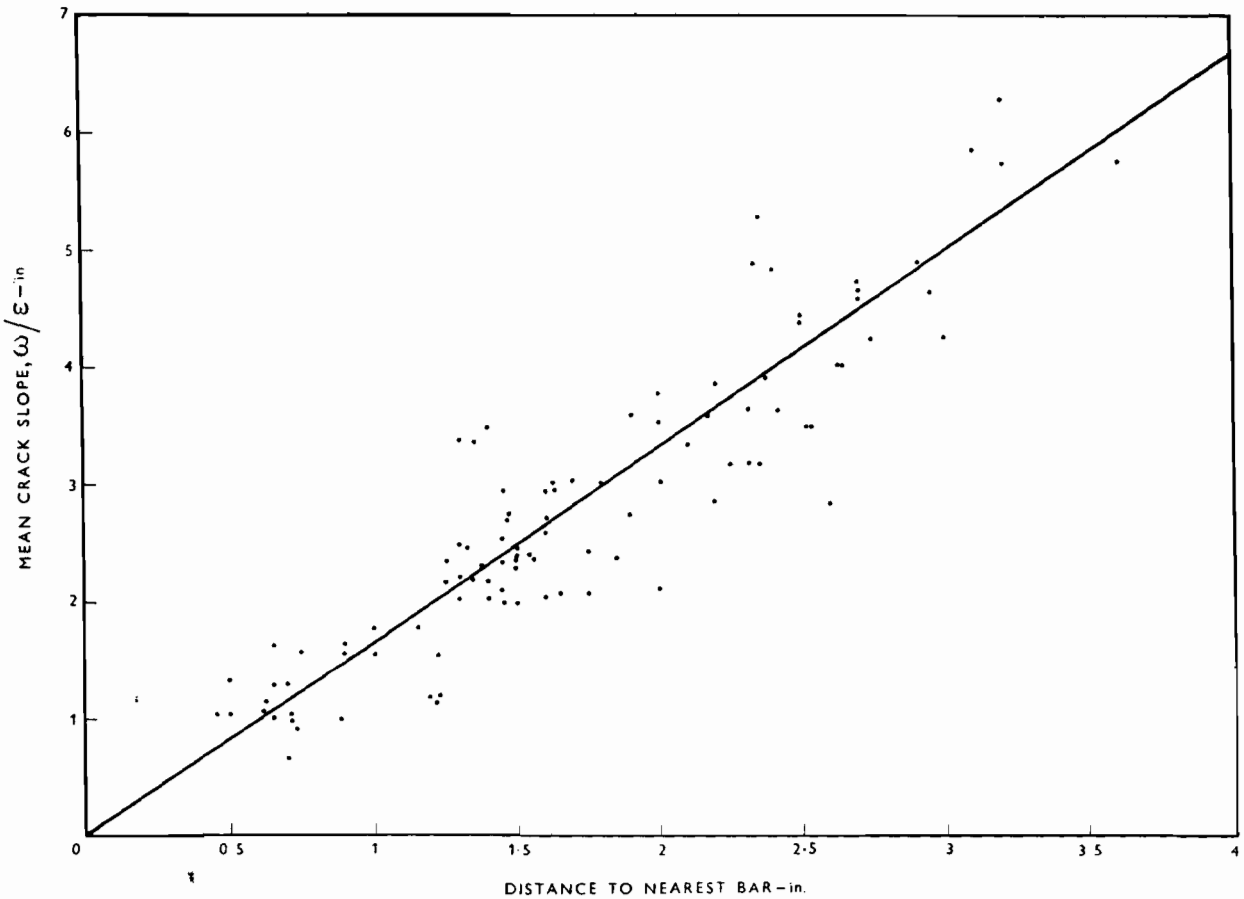

Figure 24: Experimental relationships between ω/ε and the distance of the point of measurement of a crack from nearest reinforcement (deformed steels).

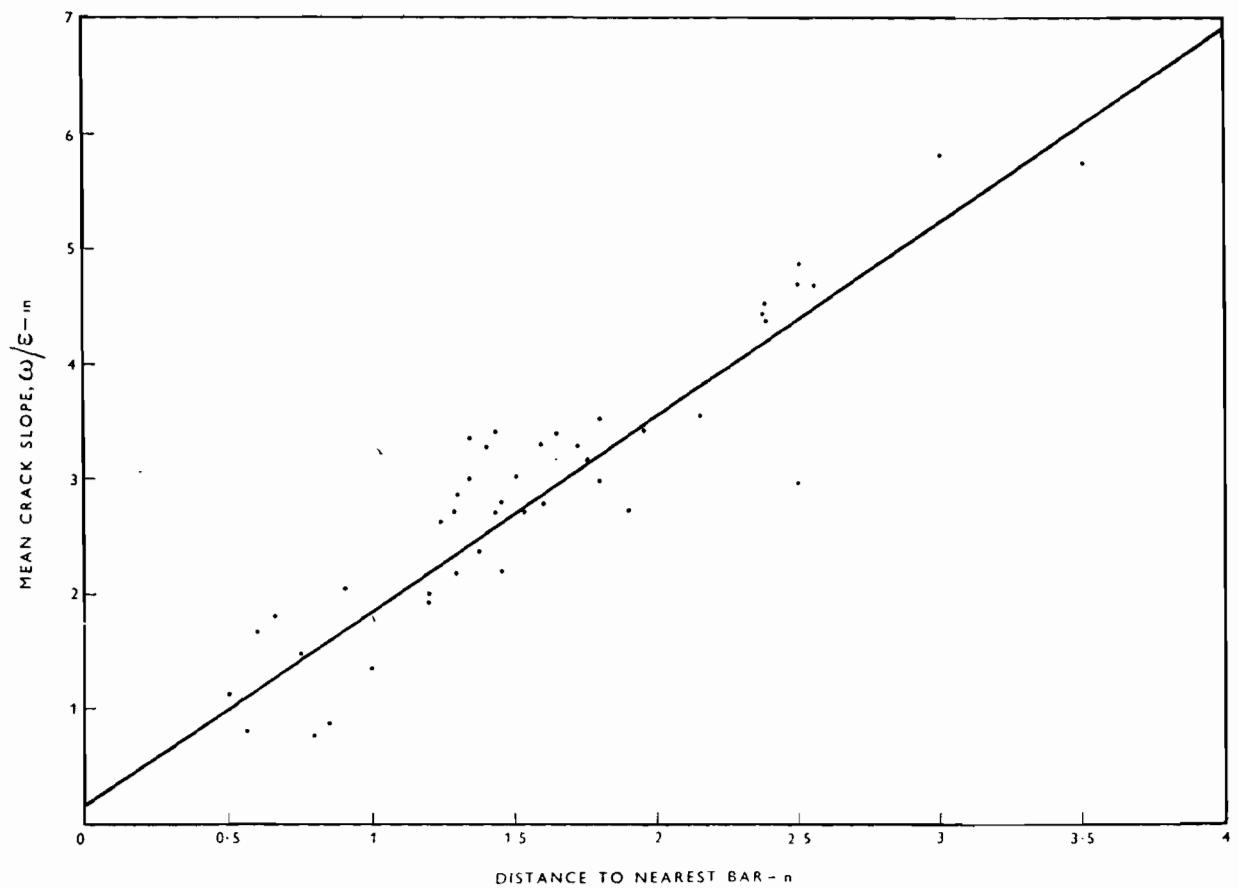

Figure 25: Experimental relationships between ω/ε and the distance of the point of measurement of a crack from nearest reinforcement (plain steels).

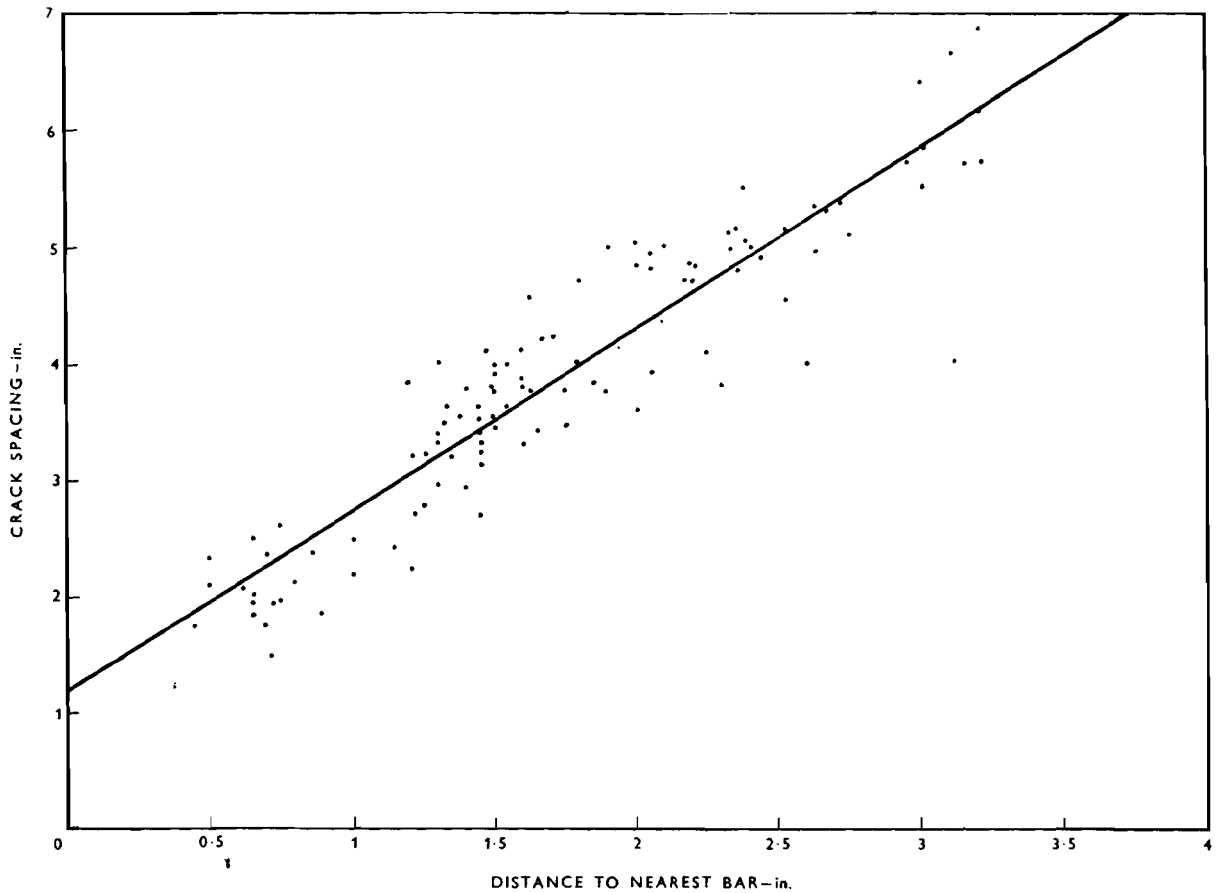

Figure 26: Experimental relationships between crack spacing and the distance of point of measurement of a crack from the nearest reinforcement (deformed steels).

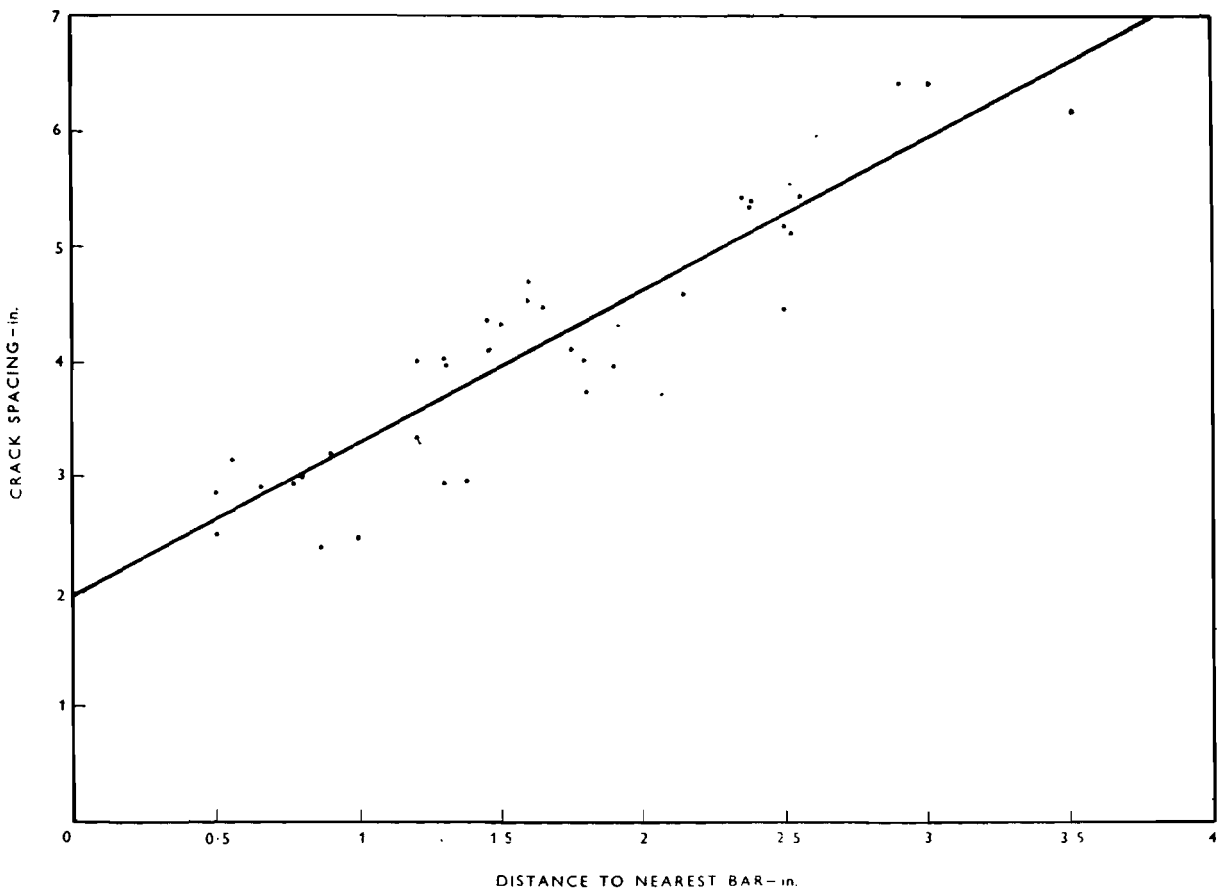

Figure 27: Experimental relationships between crack spacing and the distance of point of measurement of a crack from the nearest reinforcement (plain steels).

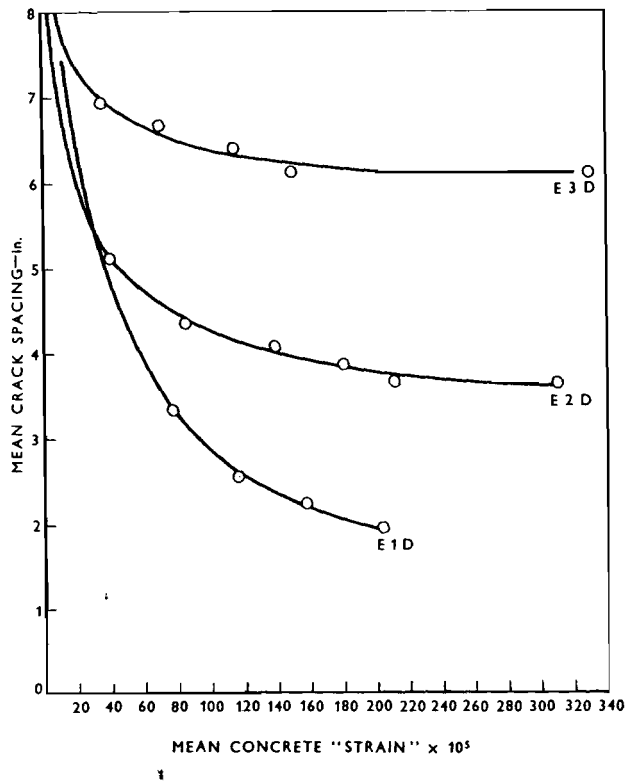

Figure 28: Development of cracking as load increases. Beams E1D, E2D and E3D.

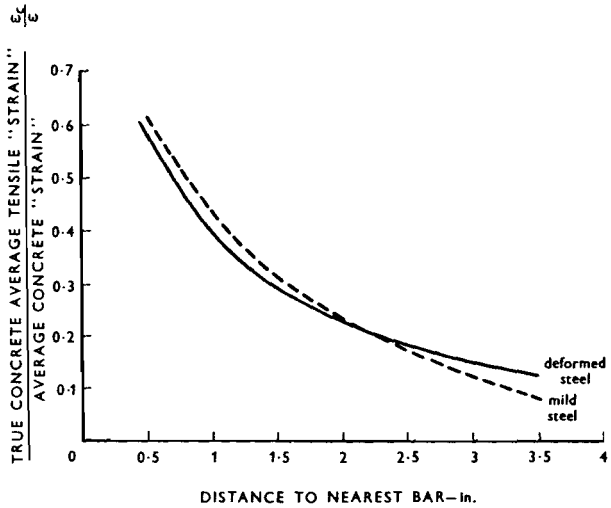

Figure 29: Relationships between strain in the concrete and distance of point of measurement of a crack from the nearest reinforcement (plain and deformed bars).

centres of two cracks $= \varepsilon S$ where ε is the average 'strain' over the 80 in. constant moment zone and S is the average crack spacing.

$$\varepsilon S = \omega + \varepsilon_c S$$

where ω is the crack width and ε_c is the true concrete strain (average over length $S - \omega$, ω negligible compared with S). Therefore

$$S - \frac{\omega}{\varepsilon} = \varepsilon_c \frac{S}{\varepsilon}$$

Thus from the graphs (using the best fit lines), further graphs, of $\varepsilon_c/\varepsilon$ against distance to bar, can be drawn as in Figure 29. It can be seen that deformed steel and plain steel gave similar curves. Both curves indicate that the actual concrete strain becomes a higher proportion of the combination of crack width and the concrete strain, ε, as the distance to the bar decreases. The concrete strain, ε_c, does not reach a limiting value when a crack pattern developes but continues to increase as ε increases and the results show that the concrete strain can, in fact, reach very high values when the cover is low. This supports the theory that the concrete adjacent to the steel is able to reach high strains before adhesion between the steel and concrete is broken down and, therefore, that cracks are likely to be wedge shaped with small (possibly zero) width at the steel-concrete interface and gradually increasing in width with increasing distance from the steel. It follows that bar type and bar diameter should have little influence on cracking, at least, until adhesion between the steel and concrete is broken down.

By referring back to the Series A1, A2 and A3, it can be seen that the smaller crack widths in Series A3 compared with A1 and A2 were probably due to the smaller bottom cover in Series A3. The ratios of the mean crack width slopes for Series A3, A2 and A1 were 1:1·21:1·27 for deformed bars and 1:1·18:1·10 for plain bars. The average difference of 20% between A3 and the other two series is very similar to the difference in cover between A3 and the other two series.

The influence of the distance from the point of measurement of a crack to the nearest bar is shown in Figure 30 which shows diagrams typical of Figures 106 to 136 in the Supplement. At each grid level the mean crack width has been plotted when the average strain in the concrete at the level of the particular grid line was a certain value. Strain values of 0·001 and 0·002 were chosen. The diagrams show the actual positions of the reinforcement bars as measured when the beams were broken after testing, and illustrate the proportionality between crack width, at a given strain, and the distance to the nearest bar. These Figures illustrate the difficulty of correlating the results of investigations by various research workers when full details of the positions of measurements of cracks and of actual bar positions are not given.

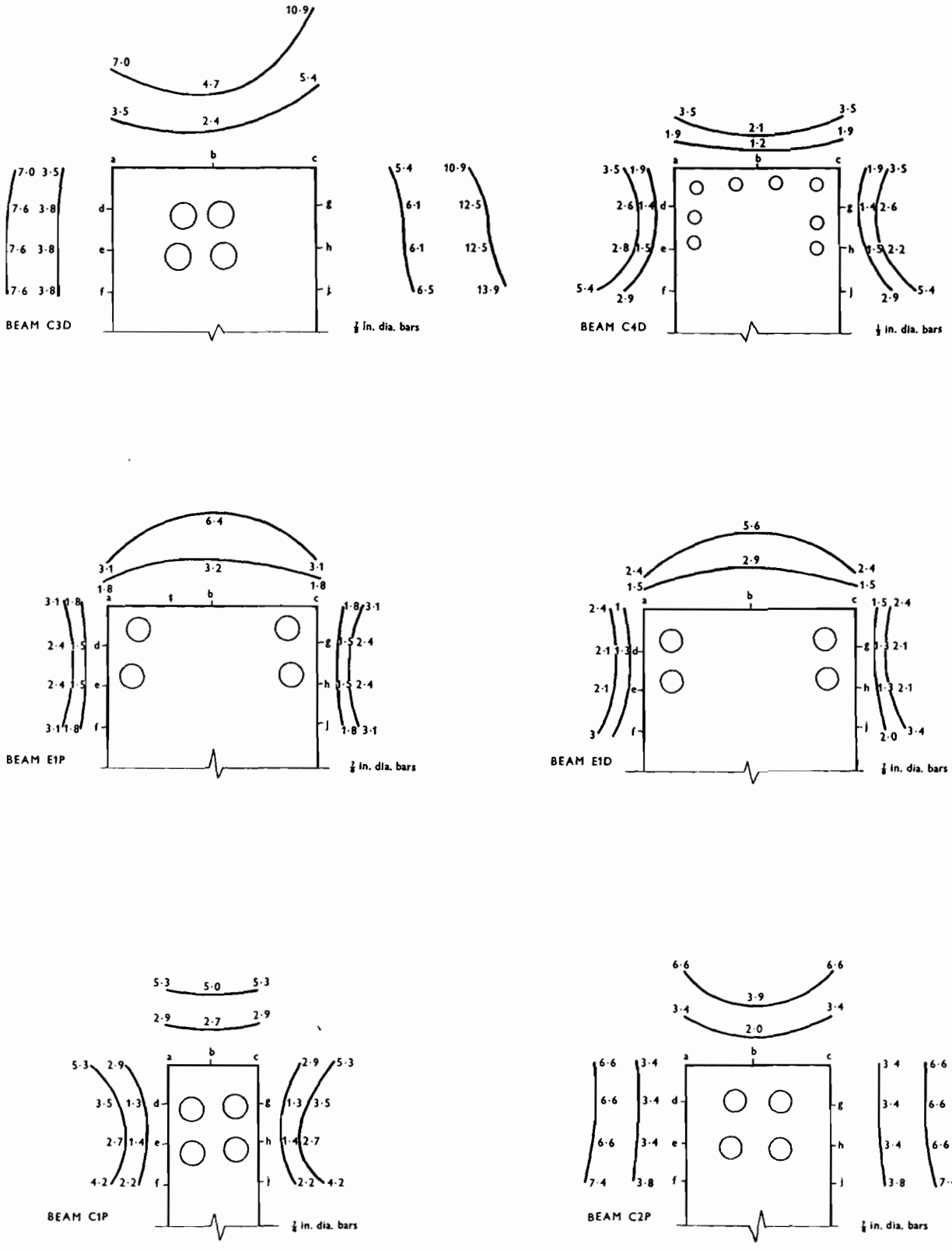

Figure 30: Influence of distance from point of measurement of a crack to the nearest bar upon crack width for six representative beams. (Values are in in. × 10^{-3} at the 100 and 200 × 10^{-5} strain levels.)

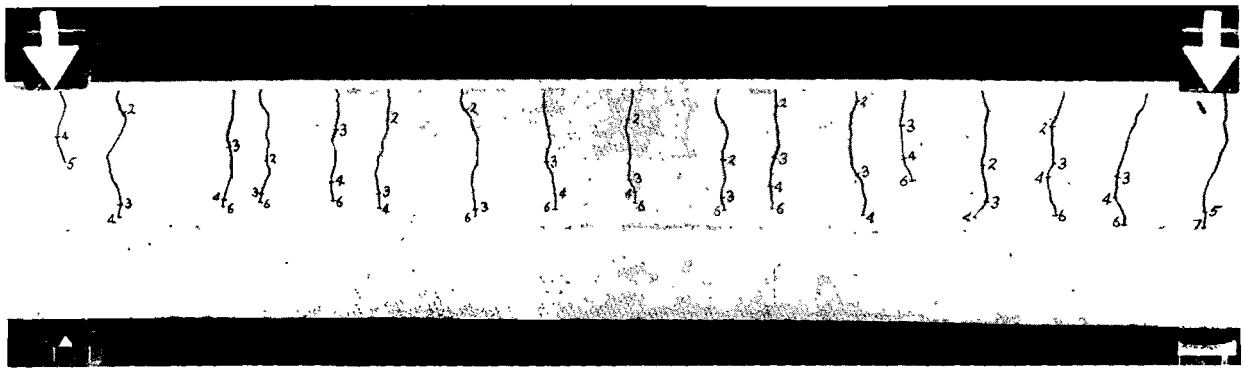

(*a*) *Beam C3P. Plain round steel, 2⅝ in. side cover.*

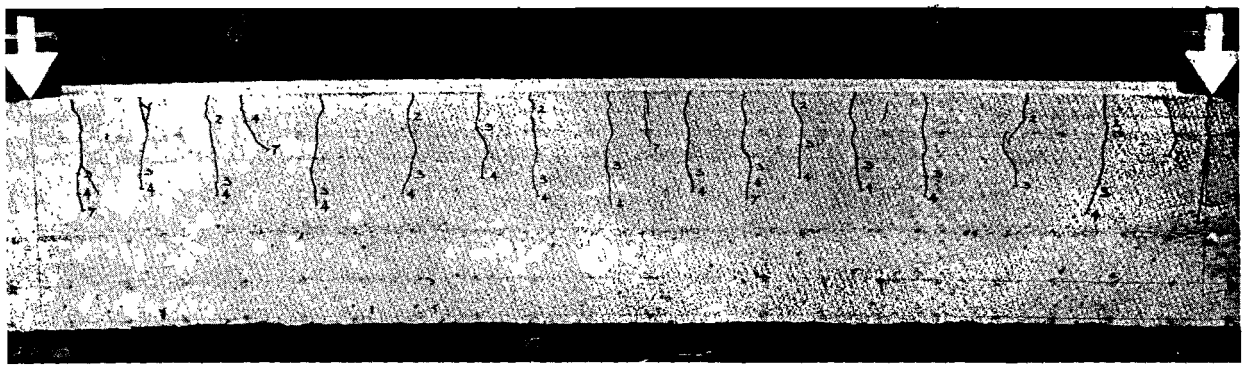

(*b*) *Beam C3D. Deformed steel, 2⅝ in. side cover.*

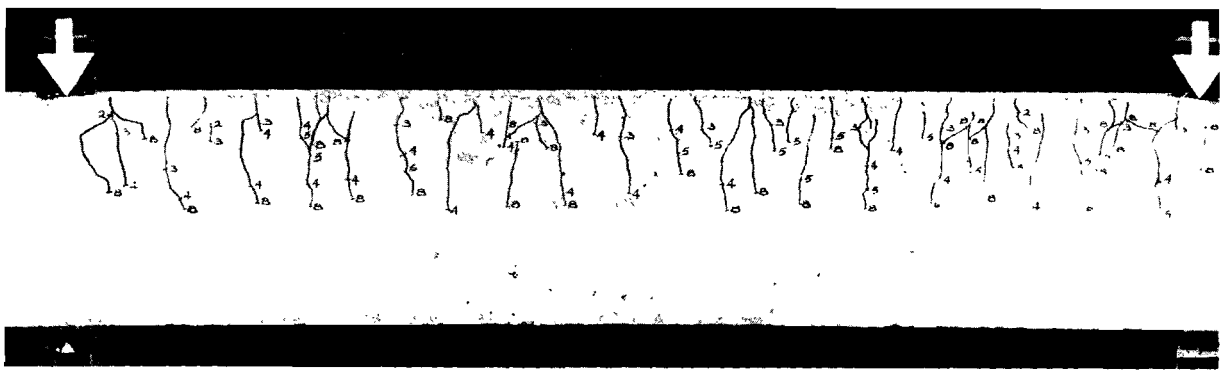

(*c*) *Beam C1P. Plain round steel, ½ in. side cover.*

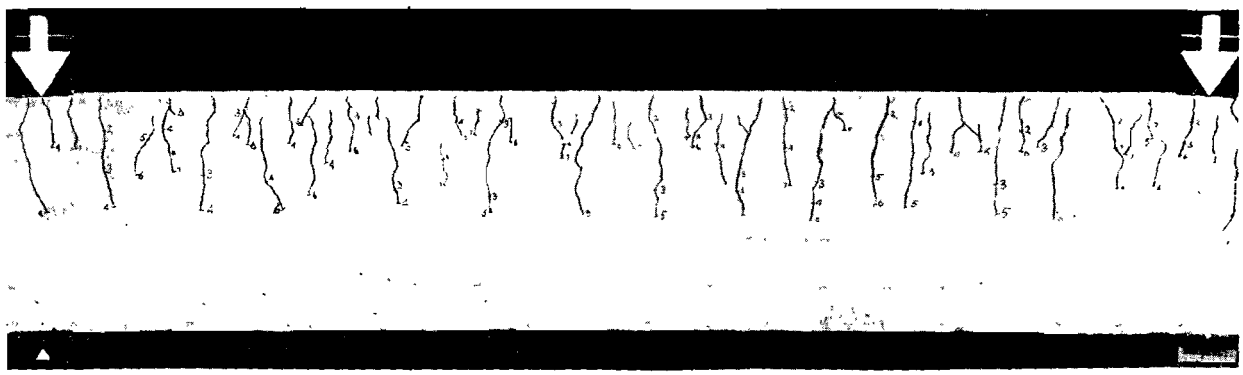

(*d*) *Beam C1D. Deformed steel, ½ in. side cover.*

Figure 31: Beams of Series C (after completion of testing).

The four photographs in Figure 31 are of beams of Series C after completion of testing and show all cracks outlined in ink. Figures 31a and 31b are of two beams with equal nominal side covers to the reinforcement ($2\frac{5}{8}$ in.) but the beam in Figure 31a has plain round reinforcement whereas the beam in Figure 31b has heavily ribbed reinforcement. Despite the difference in reinforcement the crack patterns are very similar. Figures 31c and 31d are of two other beams with equal nominal side covers (only $\frac{1}{2}$ in. in this case) and with plain round and heavily ribbed reinforcement respectively. Again the two crack patterns are very similar. However, the difference in the crack patterns between the two pairs of beams is remarkable and illustrates the effect of cover (or more precisely the distance from point of measurement of the crack to the nearest reinforcement bar) on cracking.

5: INFLUENCE OF CONCRETE STRENGTH

Three beams of Series F were made with different compacting factors (0·88, 0·92, 0·95) to give a range of concrete strengths when the beams were tested at approximately the same age. Three other beams were made with the same compacting factor (0·92) but were tested at different ages (14, 35 and 85 days). Cube strengths (Table 1) ranged from 2,825 to 4,960 lb/in^2, indirect tensile strengths (splitting cylinder) ranged from 247 to 389 lb/in^2 and the modulus of rupture from 340 to 510 lb/in^2.

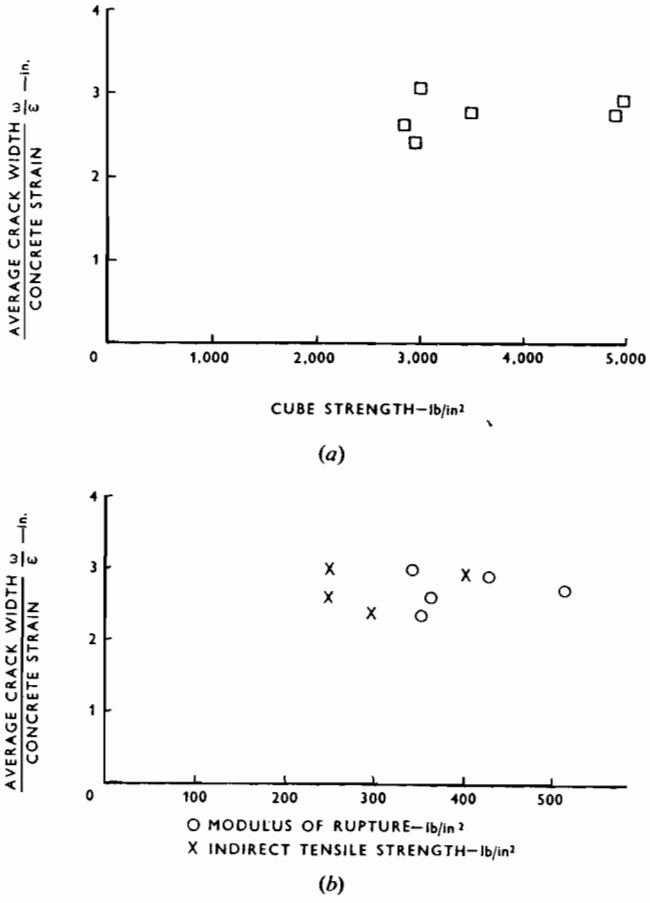

Figure 32: Influence of concrete strength on crack width.

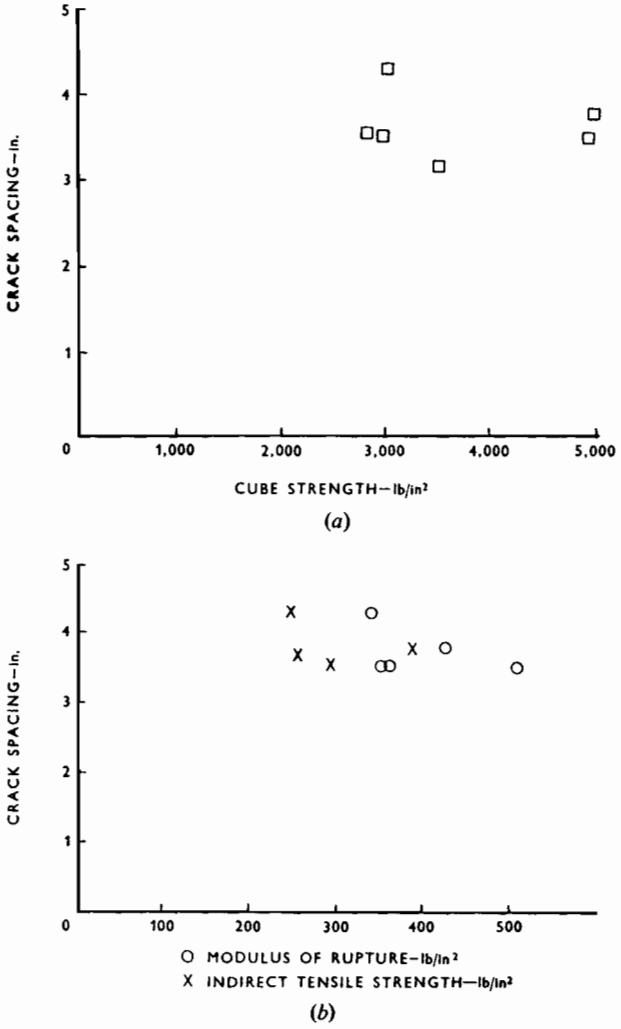

Figure 33: Influence of concrete strength on crack spacing.

The mean crack widths and maximum crack widths, both plotted against average concrete strain at the level of the measurement, are shown in Figures 69 to 74 in the Supplement. The six graphs are very similar.

In Figures 32a and 32b, the slope of the mean crack width line, ω/ε, has been plotted against cube strength and tensile strength respectively and in Figures 33a and 33b, crack spacing (when $\varepsilon \geqslant 130 \times 10^{-5}$) has been plotted against cube strength and tensile strength. No correlation between cracking and concrete strength can be observed in these graphs.

Furthermore, Student's 't' tests confirmed that all the beams in the series could have come from the same population; no values of 't' exceeded that corresponding to a 5% probability.

6: INFLUENCE OF REINFORCEMENT PERCENTAGE

The percentage of reinforcement was varied in two ways. In three beams the number of bars was varied; twelve, nine and six bars of $\frac{1}{2}$ in. diameter were used in a constant section. In three other beams the size of bar was varied; four bars of $\frac{7}{8}$, $\frac{3}{4}$ and $\frac{5}{8}$ in. diameter were used in a constant section. The investigation was made both with plain and heavily deformed steels (Series G).

No correlation between reinforcement percentage and cracking was shown, or between D/p_e (a term included in most crack prediction formulae) and cracking. A straight-line regression analysis gave a slope not significantly different from zero, indicating no correlation. Cover to the sides of the reinforcement was variable in this series but this does not appear to affect the validity of the conclusion that variation of reinforcement percentage between 1·12 and 2·29% does not influence cracking significantly.

7: INFLUENCE OF STIRRUPS

In Series B, stirrups were incorporated in four beams (two with plain steel and two with deformed steel) generally at a spacing of 6 in., which was about $1\frac{1}{2}$ times the mean crack spacing for the similar beams in Series A2. Bar layout, cover, etc., in these beams were as in Series A2.

In four other beams (two with plain steel and two with deformed steel) stirrups were also incorporated generally at 6 in. centres but the side and bottom cover was reduced from $1\frac{3}{8}$ in. to $\frac{3}{4}$ in. The effect of reducing cover in this way in a beam without stirrups would be approximately to halve the crack spacing and width. Thus a stirrup spacing of 6 in. would be about 2 to 3 times nominal mean crack spacing. In all eight beams the four stirrups adjacent to each loading point were at 4 in. centres.

If it is assumed that stirrups act as crack inducers, then the inclusion of stirrups at the mean crack spacing that would occur in an unstirruped beam should have the effect of producing cracks at uniform spacing, reducing the standard deviation. The inclusion of stirrups at a spacing greater than the normal minimum crack spacing but less than the normal mean crack spacing should decrease the crack spacing and, therefore, the crack width. The inclusion of stirrups at a spacing between the normal mean crack spacing and the normal maximum crack spacing should increase the crack spacing and the crack width because after cracks have formed at stirrups no further cracks would be able to form in the spaces between stirrups, the stirrup spacing being less than twice minimum normal crack spacing. When the stirrup spacing just exceeds the normal maximum crack spacing the resulting cracks should be regularly positioned at the stirrups and also halfway between; the spacing would be approximately the normal minimum crack spacing.

The foregoing reasoning is, of course, based on the assumption that minimum crack spacing is half the maximum crack spacing and, thus, that maximum crack spacing is 1·33 times the mean crack spacing. In fact the standard deviation of the crack widths in the first 36 beams averaged 0·415 (range 0·34 to 0·46) of the mean crack width and mean crack width was approximately proportional to mean crack spacing. Thus the maximum crack spacing, $(m + 2\sigma)$, was approximately 1·8 times the mean spacing, and the results cannot be expected to support the reasoning precisely.

Careful study of the crack patterns supports the assumption that stirrups tend to act as crack inducers and that this is more likely to be so for small cover than for large cover. In the beams with small cover there were very few cases where a stirrup did not induce a crack but in the beams with larger cover there were rather more stirrups without cracks.

Where stirrup spacing was 4 in. and the cover such that the normal mean crack spacing would be 4 in. there was some evidence that the stirrups reduced the variability of crack spacing. Where the stirrup spacing was 6 in. in the same beams, that is between the normal mean and maximum crack spacings, cracks formed at most stirrups and additional cracks formed between approximately half the pairs of stirrups.

In the beams where the cover was small the normal mean crack spacing would have been about 2 in. The stirrup spacings were thus multiples of the mean crack spacing and either one or two cracks formed between stirrups in addition to the cracks at stirrups.

Many more tests would be necessary to give statistically acceptable evidence of the influence of stirrup spacing on cracking.

8: INFLUENCE OF CURING

Three beams cast together were subsequently treated in different ways. One was allowed to dry in the laboratory after one day, one was kept moist under polythene for one week and then allowed to dry and the other was kept under damp hessian and polythene for a month. The three beams were tested when approximately one month old. Shrinkage control specimens kept with the beams had shrunk approximately in the ratios 9:5:1 at the time the beams were tested.

Comparison of the graphs of mean crack width against strain for the three beams shows no significant differences, either in slope or intercept on the axes, and 't' tests indicate that the three beams were from the same population. Each beam was also compared with Series A2 and found to be similar; no values of 't' exceeded the 5% probability level.

9: INFLUENCE OF CASTING UPSIDE DOWN

Four beams were cast together, two with the tension zone at the bottom of the mould and two with the tension zone at the top of the mould. This small sample of beams gave no clear indication of the effect of the parameter being studied; variation between similar beams was of the same order as the variation between comparison beams.

10: INFLUENCE OF SHEAR SPANS

Three beams were cast together and tested with shear spans of 30, 42 and 60 in. and the uniform bending moment zones were thus 120, 96 and 60 in. respectively. Shear reinforcement in the shear spans consisted of an equal number of stirrups in each, the spacing being reduced as the shear span was reduced.

In these beams crack widths and spacings were measured in the shear spans as well as in the uniform bending zone. Strain measurements were made along the whole length of the beam.

The slopes of the graphs of mean crack width against average concrete strain for the the uniform bending moment zones were compared by means of 't' tests; each of the three beams was compared with the remaining two and each of the three beams was also compared with the population of twelve beams in Series A2. Except for comparison between beam K1 (30 in. shear span) and Series A2, all the tests indicated that the beams came from the same population; 't' values did not exceed the 5% probability level. Comparison between K1 andSeries A2 gave a value of 't' at the level of uncertainty.

Measurements in the shear spans were treated in the same general way as those in the uniform moment zones. The shear spans were divided into ten sections and the mean crack widths in each section plotted against the mean concrete strain in the section. In all cases the slope of the graph was slightly less than that for the uniform moment zone; the average ratio was 1:1·1 but this is only a rough indication of the possible difference between shear span and uniform moment zone.

At high loads (steel stress greater than 50,000 lb/in^2) the cracks in the shear spans became inclined and were then generally wider than the cracks in the uniform bending moment zone.

General observations arising from the results

1: RELATIONSHIPS BETWEEN CRACK SPACING AND CRACK WIDTH

The relationship between crack spacing and crack width is involved in the theories of cracking and is often considered in the examination of research into the phenomenon of cracking. The typical assumption,

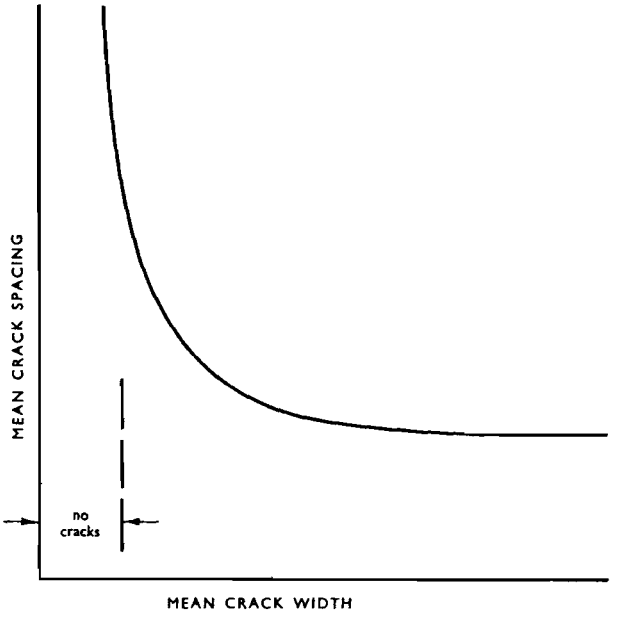

Figure 34: Relationship between crack width and crack spacing at a certain level on the beam.

or statement, that crack width is proportional to crack spacing is, however, very loose and must be more precisely defined. It must, for example, be established whether the relationship applies at all loads on the beam or at all positions (distances from the neutral axis) or whether something more specific is meant.

As load is applied to a beam for the first time the relationship between mean crack spacing and mean crack width at a particular level on the beam (say the centre of the soffit, or the level of the centroid of the reinforcement) must clearly be of the type illustrated in Figure 34. At zero load, crack spacing is infinite and crack width zero. At a certain load, cracks begin to form and, as the load is increased, the crack spacing tends towards a limiting minimum value while the crack width continues to increase. The crack width is a function of the stress in the reinforcement and, therefore, of the average 'strain' in the concrete at the level of the reinforcement; in fact, direct proportionality between crack width and the 'strain' has been demonstrated. Thus, the mean crack width axis in Figure 34 can also be considered as the 'average strain' axis. (Figure 26 is of this type of relationship.) Now strain also increases with increasing distance from the neutral axis of a beam and thus the distribution of crack spacing between the neutral axis and the soffit of a beam should, if other factors have no influence, be as in Figure 34. In a small zone below the neutral axis there would be no cracks. In a zone of considerable height above the soffit of the beam the crack spacing would be constant. Between the zones there would be a rapid transition from a certain minimum crack spacing to infinite crack spacing. In other words, most cracks present at the soffit of a

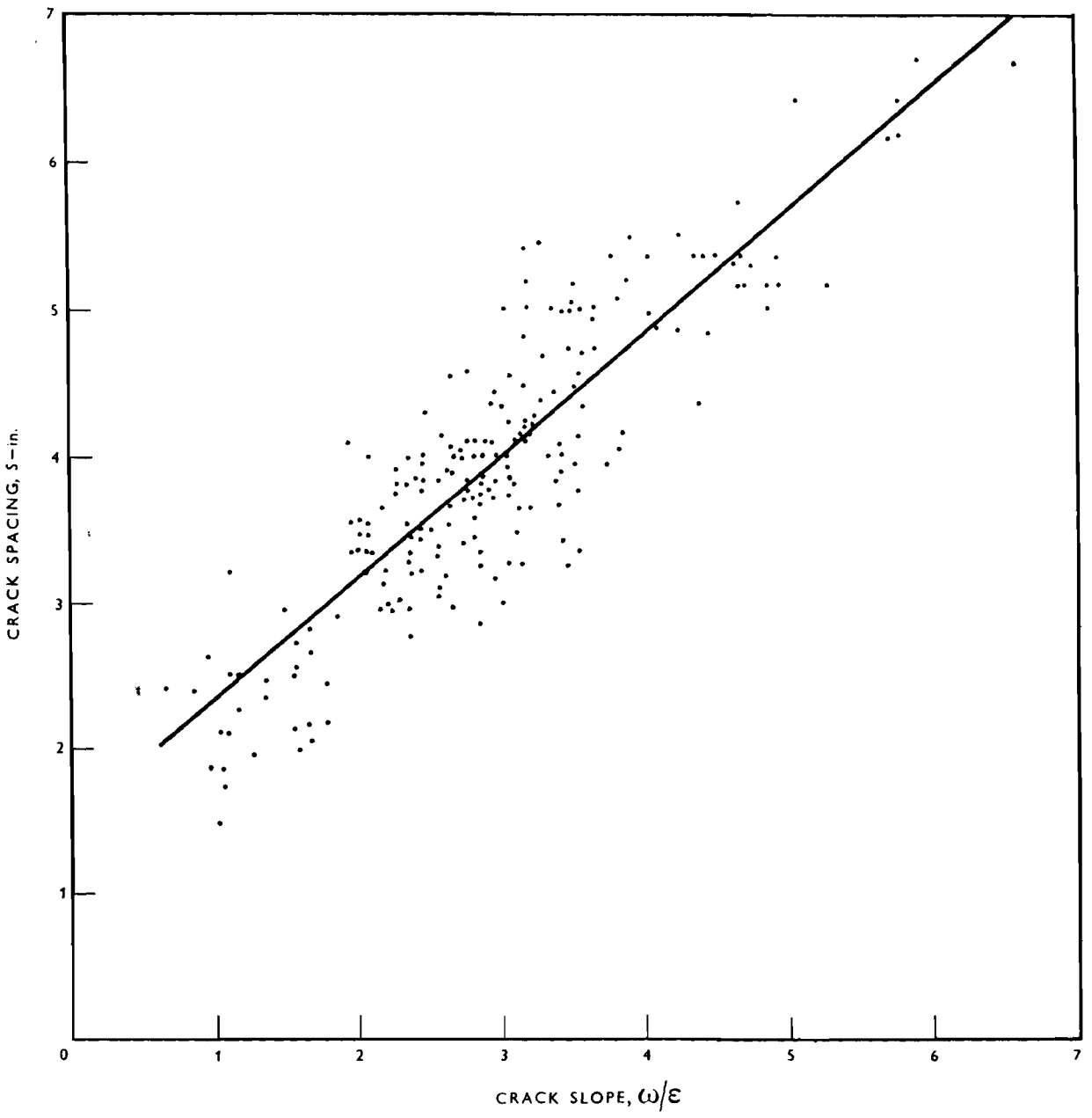

Figure 35: Relationship between cracking spacing and mean crack slope.

beam extend to within a small distance of the neutral axis, a few extend slightly further than the majority and a few terminate slightly lower than the majority. This pattern of cracking is very common, particularly in beams where the depth of the tension zone is not large compared with the side cover to the reinforcement.

In beams where the cover to the reinforcement is small, the variation in the distance of the point of measurement of a crack to the nearest bar is considerable within the tension zone of the beam. As shown by this investigation, this variation has a very considerable influence on crack spacing and on crack width and in beams with small cover to the reinforcement there are many cracks in the region of the reinforcement which do not penetrate far towards the neutral axis.

The proportionality between crack width and crack spacing that is assumed in the ' classical ' theory refers to the relationship that exists at a load when the crack pattern is completely formed. It is simply a statement that for a given set of conditions (namely, specified bar type, bar size, effective reinforcement ratio and steel stress) the crack width is inversely proportional to the number of cracks that exist. It is, of course, implicit that *all* cracks are included in the relationship; there may be no arbitrary division between ' major ' and ' minor ' or ' primary ' and ' secondary ' cracks.

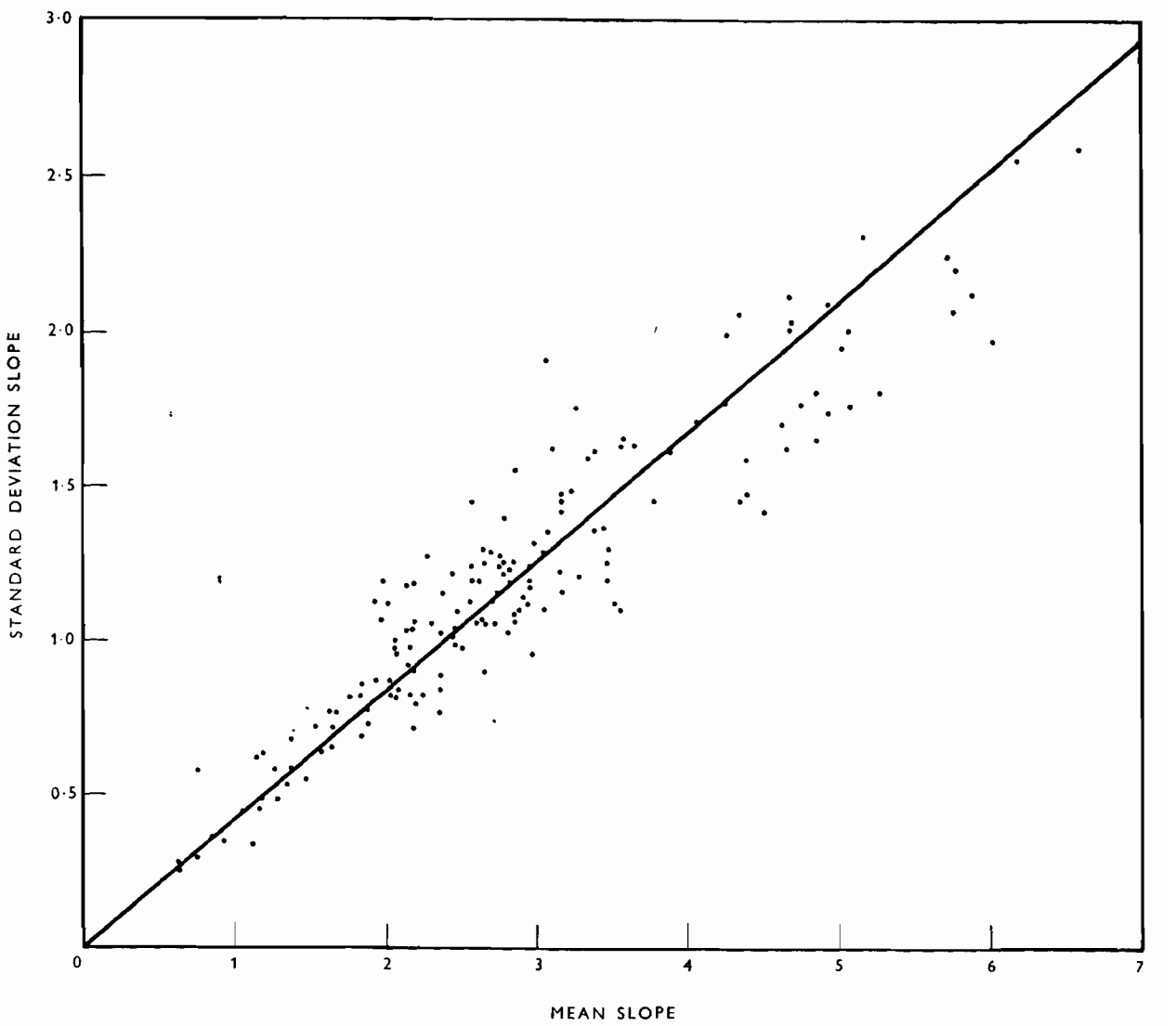

Figure 36: Relationship between mean crack slope and standard deviation slope.

For the present investigation Figure 35 shows the graph of the crack pitch existing when the average concrete strain exceeded 130×10^{-5} at the level considered, plotted against the slopes of graphs of mean crack width against average concrete strain for the level considered. Despite the scatter of results there is no reason to doubt the linear relationship.

2: THE RELATIONSHIP BETWEEN MEAN CRACK WIDTH AND STANDARD DEVIATION OF CRACK WIDTHS

The classical theory suggests that the relationship between maximum crack width and mean crack width should be $\omega_{max} = 1{\cdot}33\ \omega_{mean.}$ In fact a greater range than this would be expected owing to factors not considered in the theory.

In Figure 36, the slopes of graphs of mean crack width against average concrete strain are plotted against those of standard deviation against average strain. The best-fit line from the regression analysis does not pass through the origin and a best-fit line forced through the origin has been plotted; the equation to this is

standard deviation = $0{\cdot}416 \times$ mean crack width.

A value of mean + 2·4 standard deviations is exceeded in a normal distribution approximately once in a hundred events. Thus we can say that a value of

$\omega_{max} = \omega_{mean} + (2{\cdot}4 \times 0{\cdot}416)\ \omega_{mean}$ i.e., $\omega_{max} = 2{\cdot}0\ \omega_{mean}$ will only be exceeded approximately once in a 100 cracks.

Suggested crack width formula

From the relationship between mean crack width and distance to nearest bar c, (see Figure 24) we have, for deformed bars:

$$\omega_{mean} = 1{\cdot}67 c\varepsilon$$

where ε is the average ' strain ' in the concrete at the level of the crack measurement.

Thus $\omega_{max} = 2\ \omega_{mean}$
$= 3{\cdot}3 c\varepsilon$

Then, if d = distance from the compression face of the beam to the level of the crack measurement
d_n = distance of the neutral axis from the compression face of the beam
d_1 = distance of the centroid of the tension reinforcement from the compression face of the beam
ε_s = average ' strain ' in the concrete at the level of the centroid of the reinforcement,

we have $\omega_{max} = 3{\cdot}3\ c\ \varepsilon_s \left(\frac{d - d_n}{d_1 - d_n}\right)$

or $\omega_{max} = 3{\cdot}3 c \frac{f_s}{E_s} \left(\frac{d - d_n}{d_1 - d_n}\right)$

For plain round bars crack widths were, on average, 20% greater than for deformed bars. Thus for plain round bars

$$\omega_{max} = 4{\cdot}0 c \frac{f_s}{E_s} \left(\frac{d - d_n}{d_1 - d_n}\right)$$

The formulae predict maximum crack widths, at the level of the centroid of the reinforcement, as calculated in Table 15.

TABLE 15: **Predicted maximum crack widths in reinforced concrete beams.**

Stress in reinforcement	Maximum crack width at level of centroid of reinforcement (in. × 10^{-3})					
	Plain round steel			Deformed steel		
	Side cover (in.)			Side cover (in.)		
(lb/in²)	1	1½	2	1	1½	2
20,000	2·7	4·0	5·3	2·2	3·3	4·4
30,000	4·0	6·0	8·0	3·3	5·0	6·6
33,000	4·4	6·6	8·8	3·6	5·5	7·2

At the soffit of the beam crack widths slightly greater than the values in Table 15 would occur.

Comparison between typical existing crack prediction formulae and the proposed formula

Existing crack prediction formulae generally include, as major parameters, bar diameter and effective reinforcement ratio and exclude the cover to the reinforcement. The proposed formulae exclude bar diameter and effective reinforcement ratio and include the cover to the reinforcement.

The proposed CEB equation is

$$\omega_{max} = \left(4{\cdot}5 + \frac{0{\cdot}4}{p_e}\right) \frac{Df_s}{K_2}$$

In Figure 37 the maximum crack width has been plotted against $(4{\cdot}5 + 0{\cdot}4/p_e)D$ for a value of f_s of 40,000 lb/in² and for deformed bars only (i.e. K_2 is constant) for reported results by Hognestad[6], Kaar and Mattock[7], and for all the deformed bar beams of the main C & C A investigation. To ensure that comparisons are made on a reasonably uniform basis, only measurements made at the level of the centroid of the reinforcement are plotted. It must, however, be pointed out that the point of maximum width of a crack is not necessarily at the level of the centroid of the reinforcement; indeed it is unlikely to be. The correlation between the theoretical line and the reported results, in Figure 37, is poor and it appears unlikely that it would be significantly improved if it were possible to plot crack widths for points other than the level of the centroid of the reinforcement.

The empirical equation derived as a result of the PCA investigation[7] is $\omega_{max} = 0{\cdot}115\ \sqrt[4]{A}\ f_s \times 10^{-6}$ in. where $A = A_e$ divided by number of bars, described as " area of concrete surrounding each bar ". In Figure 38 the maximum crack width at the steel level has been plotted against $\sqrt[4]{A}$ for $f_s = 40{,}000$ lb/in² for results reported by Hognestad[6], Kaar and Mattock[7] and all the deformed bar beams of the main C & C A investigation. The correlation is again poor.

The formula for deformed steel proposed as a result of the C & C A investigation is

$$\omega_{max} = 3{\cdot}3 c \frac{f_s}{E_s} \left(\frac{d - d_n}{d_1 - d_n}\right)$$

In most cases previously reported work does not include enough information to permit direct comparison between the results and this equation; either the cover to the reinforcement is not specified (or not measured) or the position of the crack measurement is not detailed. However, the C & C A investigation and theory indicate direct proportionality between ultimate mean crack spacing at the level of the centroid of the reinforcement and the side cover to the reinforcement. The ultimate mean crack spacings can be deduced from the photographs shown in the reports on many previous investigations and in Figure 39 they are plotted against side cover to the reinforcement (stated

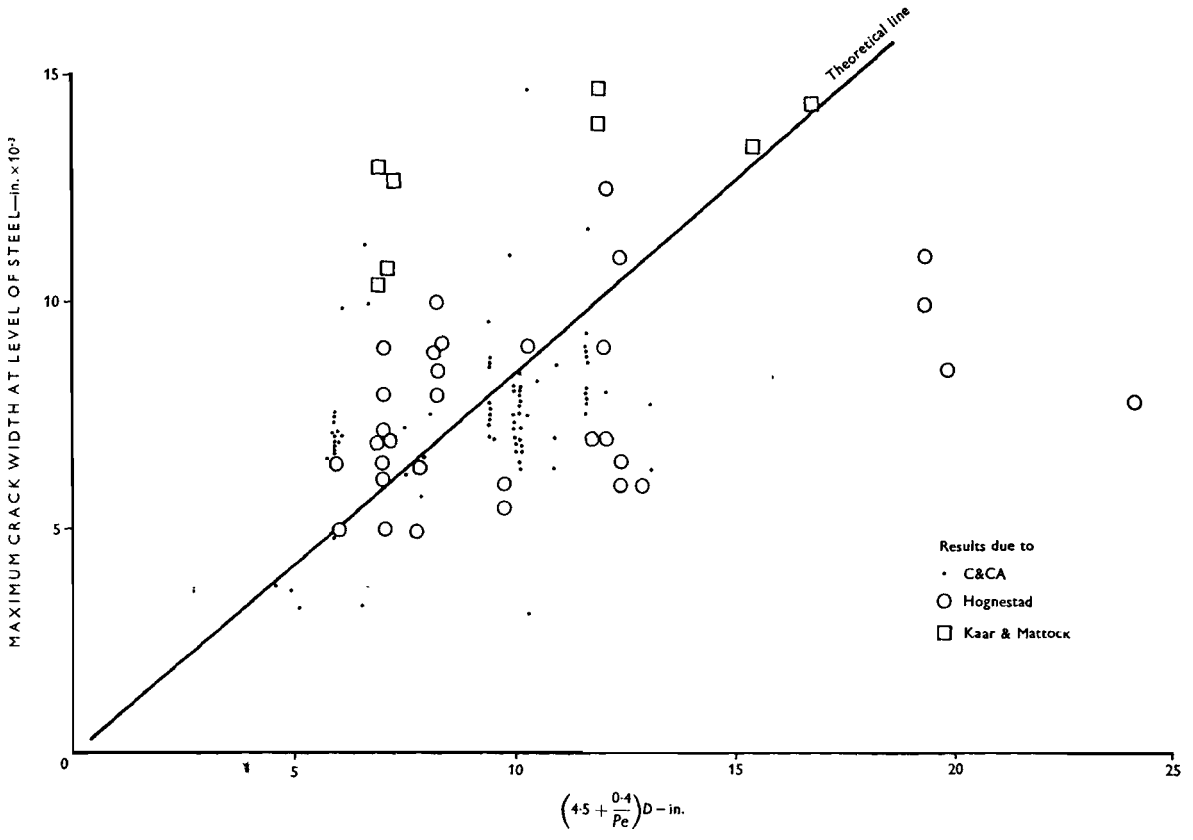

Figure 37: Comparison between various reported maximum crack widths and the CEB formula for a steel stress of 40,000 lb/in².

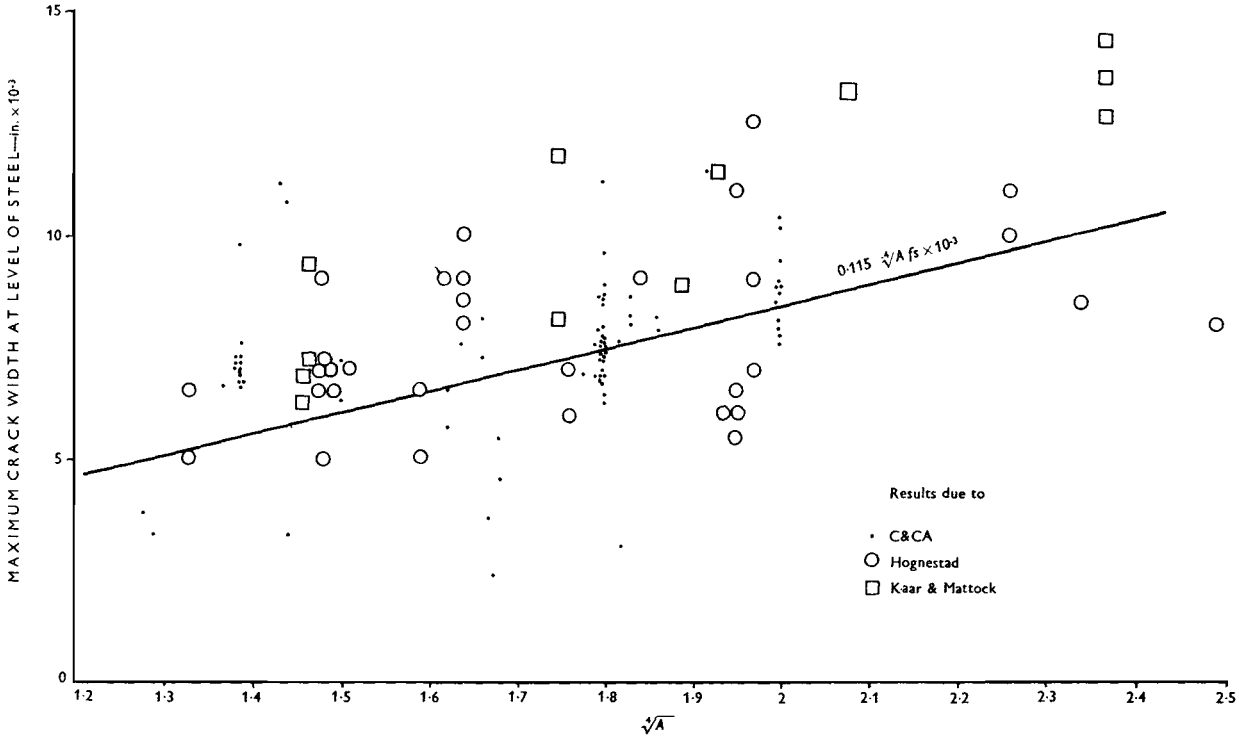

Figure 38: Comparison between various reported maximum crack widths and the PCA formula for a steel stress of 40,000 lb/in².

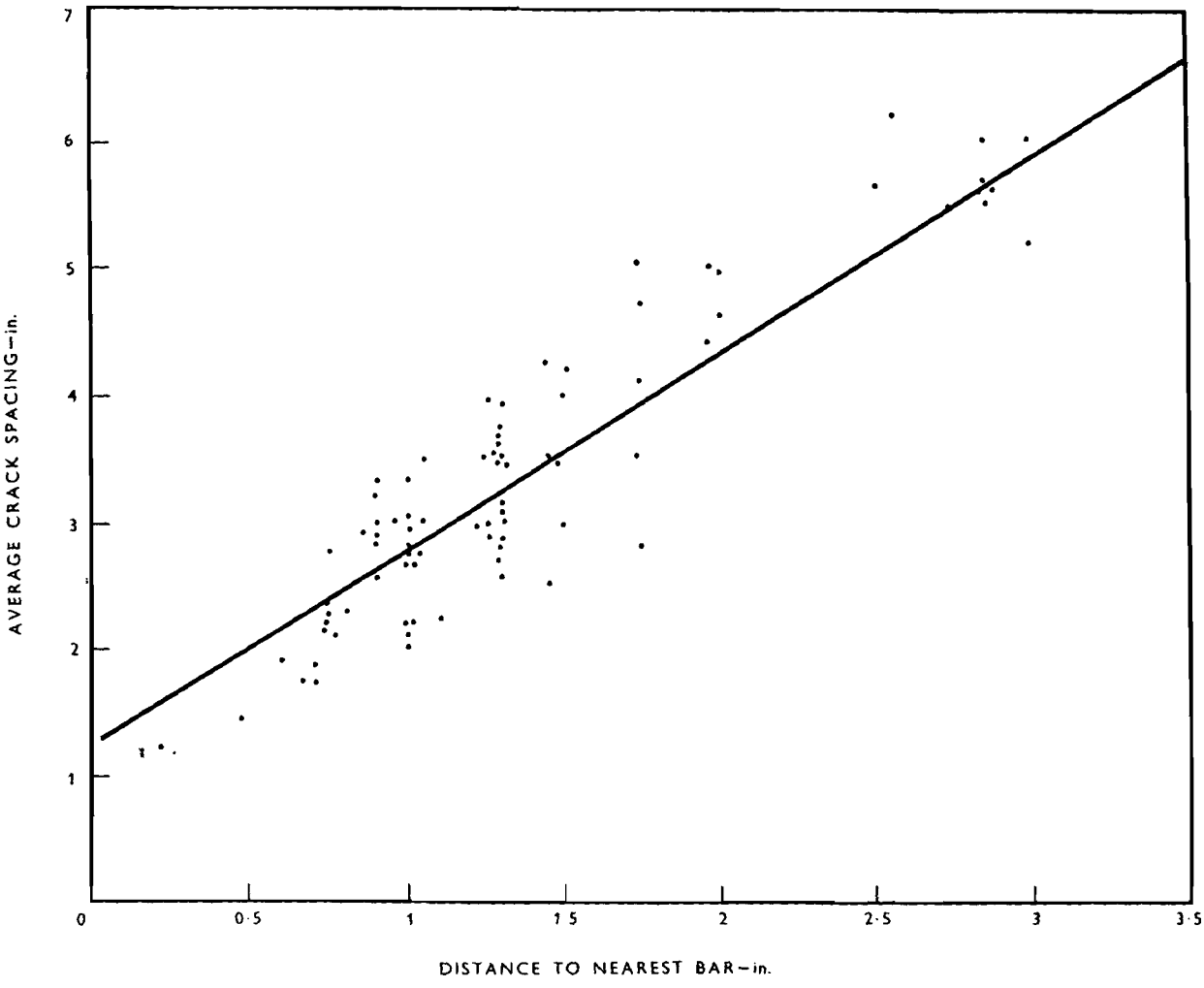

Figure 39: Ultimate mean crack spacings at the level of the centroid of reinforcement plotted against the side cover to the reinforcement, for various reported investigations.

or assumed). A linear relationship is apparent. The line plotted in Figure 39 is the best-fit regression line for the main C & C A investigation (deformed steel only) and the fit of the various experimental results and this line is good.

Conclusions

From this investigation into crack spacing and crack width in uniform bending moment zones in rectangular, or near-rectangular, beams the following conclusions are drawn.

(1) The distribution of crack widths is Gaussian and the standard deviation averages 0·42 times the mean crack width. Thus one crack in a hundred can be expected to exceed a width of twice the mean crack width.

(2) There is a linear relationship between crack width and stress in the tension reinforcement.

(3) Within the effective tension zone of a beam (i.e. the area of concrete with the same centroid as the reinforcement) the width of a crack is directly proportional to the distance from the point of measurement of the crack to the surface of the nearest reinforcement bar.

(4) The width of a crack is, within the effective tension zone, proportional to the distance of the point of measurement below the neutral axis of the beam.

(5) There is a linear relationship between the ultimate mean crack spacing and the distance of the point of measurement of the cracks from the nearest reinforcement.

(6) Within the range of crack widths normally considered acceptable in reinforced concrete, the type of reinforcing steel has little influence on the crack width. In beams reinforced with plain round mild steel the mean crack width may, on average, be 20% greater than that in beams reinforced with deformed bars (including square twisted bars) at the same steel stress. However, other factors produce differences between nom-

inally identical beams greater than the difference due to bar type and thus the mean crack width in a deformed steel beam may be greater than that in a plain steel beam at the same stress.

(7) There is no significant difference between the crack control characteristics of any of the deformed steels tested, including square twisted steel.

(8) There is no significant difference between the crack control characteristics of a small number of large bars and a large number of small bars of the same total cross-sectional area if the cover to the bars is the same.

(9) The investigation produced no evidence that variation of the percentage of reinforcement, within the range 0·85 to 2·29%, has a significant influence on cracking at a given steel stress.

(10) Stirrups act as crack inducers, particularly when the concrete cover is small and it is possible that some measure of control over crack spacing may be obtained by judicious spacing of the stirrups.

(11) The investigation produced no evidence that variation of concrete strength or of curing conditions, whether the beam was cast with the tension zone at the bottom or the top of the mould, or variation of the length of the shear span have a significant effect on cracking.

(12) Because the effect of variation in the cover to the reinforcement on the width and spacing of cracks is overwhelming, any crack prediction formula that does not include this parameter cannot be generally applicable. Moreover the effect of variation of bar size and bar type is greatly exaggerated in most formulae. The formula for the prediction of maximum crack width at present in the Recommendations for International Code of Practice for Reinforced Concrete[8] predicted a ratio of 1:4 in the maximum crack widths for two types of beam (Type A1, plain steel and Type A3, deformed steel) whereas the ratio that occurred was 1:1·2. In another case, the formula predicted identical maximum crack widths in two types of beam (Type E1 and Type E3) whereas the maximum crack widths were actually in the ratio 1:5·8.

(13) From this investigation the following formula, for the prediction of the maximum crack width on the surface of the effective tension zone, has been derived.

$$\omega_{max} = Kc\frac{f_s}{E_s}\left(\frac{d - d_n}{d_1 - d_n}\right)$$

where c = the distance of the point of measurement of the crack from the surface of the nearest main reinforcement bar

d = the distance from the compression face of the section to the point of measurement of the crack

d_1 = the distance from the compression face of the section to the centroid of the main tension reinforcement

d_n = the distance of the neutral axis from the compression face of the beam

f_s = the mean stress in the reinforcement

E_s = the modulus of elasticity of the reinforcement

K = a constant of value 3·3 for deformed bars and 4·0 for plain round bars.

For prediction of the maximum crack width at the level of the centroid of the reinforcement the formula reduces to

$$\omega_{max} = Kc\frac{f_s}{E_s}$$

(14) The proportionality between crack width on the surface of the concrete and the distance of the point of measurement of the crack from the nearest reinforcement can be explained by the hypothesis that cracks taper from a certain width on the surface of the beam to approximately zero width at the steel-concrete interface. This implies that adhesion between the steel and concrete does not break down significantly within the range of stresses normally used in reinforced concrete design and that the width of a crack is basically a function of the elastic recovery of the concrete between cracks and of the restraining effect of the nearby reinforcement.

ACKNOWLEDGEMENTS

This research was initiated and carried out by the Structural Design Research Department of the Cement and Concrete Association under the general direction of Dr R. E. Rowe. The research team was led and supervised by G. D. Base.

Valuable assistance in the programming and interpretation of this project was given by a Steering Panel comprising the following members:

Dr S. C. C. Bate, BSc(Eng), PhD, AMICE

Mr H. G. Cousins, BSc(Eng), MICE, MIStructE

Dr K. Hajnal-Kónyi, DEng, FASCE, MICE, MIStructE

Mr N. P. Roberts, BSc, AMICE

Thanks are also due to the following colleagues of the authors for their individual contributions to the project: Mr B. C. Best (advice on statistics); Mrs S. Pitcher (computer operator); Mr R. Lunn (vacation student for twelve months); Mr T. Pearce and Mr V. Dent (technicians).

REFERENCES

1. WATSTEIN, D. and PARSONS, D. E. Width and spacing of tensile cracks in axially reinforced concrete cylinders. *Journal of Research of the National Bureau of Standards.* Vol. 31, No. R.P.545. July 1943. pp. 1–24.

2. RILEM. *Proceedings of the Symposium on Bond and Crack Formation in Reinforced Concrete*, Stockholm 1957.
3. COMITE EUROPEEN DU BETON. *Report of Commission No. 4a on Cracking*. Bulletin d'information No. 12, C.E.B. Permanent Secretariat, Paris. February 1959. pp. 28.
4. TIMOSHENKO, S. and GOODIER, J. N. *Theory of elasticity*. 2nd Edition, New York, McGraw-Hill Book Co., Inc. 1951. pp. 506.
5. BEEBY, A. Technical Report to be published by the Cement and Concrete Association.
6. HOGNESTAD, P. E. High strength bars as concrete reinforcement. Part 2. Control of flexural cracking. *Journal of the Portland Cement Association Research and Development Laboratories*. Vol. 4, No. 1. January 1962. pp. 46–63.
7. KAAR, P. H. and MATTOCK, A. H. High strength bars as concrete reinforcement. Part 4. Control of cracking. *Journal of the Portland Cement Association Research and Development Laboratories*. Vol. 5, No. 1. January 1963. pp. 15–38.
8. COMITE EUROPEEN DU BETON. *Recommendations for an international code of practice for reinforced concrete*. London, American Concrete Institute and Cement and Concrete Association, 1964. pp. 156.